REPUBLIC OF TURKEY
ADANA ALPARSLAN TÜRKEŞ SCIENCE AND TECHNOLOGY UNIVERSITY

GRADUATE SCHOOL OF NATURAL AND APPLIED SCIENCES
DEPARTMENT OF MECHANICAL ENGINEERING

DESIGN AND ANALYSIS OF OIL SEPERATOR TANK USED IN SCREW TYPE COMPRESSOR SYSTEMS

VOLKAN GEZGİNCİ
MASTER OF SCIENCE

ADANA 2022

REPUBLIC OF TURKEY
ADANA ALPARSLAN TÜRKEŞ SCIENCE AND TECHNOLOGY UNIVERSITY

GRADUATE SCHOOL OF NATURAL AND APPLIED SCIENCES
DEPARTMENT OF MECHANICAL ENGINEERING

DESIGN AND ANALYSIS OF OIL SEPERATOR TANK USED IN SCREW TYPE COMPRESSOR SYSTEMS

VOLKAN GEZGİNCİ
MASTER OF SCIENCE

SUPERVISOR
Asst. Prof. Dr. Cem BOĞA

ADANA 2022

I hereby declare that all information in this thesis has been obtained and presented in accordance with academic rules and ethical conduct. I also declare that, as required by these rules and conduct, I have fully cited and referenced all information that is not original to this work.

[Signature]

Volkan GEZGİNCİ

ABSTRACT

DESIGN AND ANALYSIS OF OIL SEPERATOR TANK USED IN SCREW TYPE COMPRESSOR SYSTEMS

Volkan GEZGİNCİ
Department of Mechanical Engineering
Supervisor: Asst. Prof. Dr. Cem BOĞA
January 2022, 73 pages

Pressure vessels are geometrically cylindrical, spherical, or conical work equipment used for the storage and transportation of various liquids and gases with an internal pressure of more than 0.5 bar, which has a key role in all compressor systems. Damages that may occur if pressure vessels are not designed and produced correctly or used incorrectly due to working conditions can cause serious damage to the environment and employees. The focus of this study is to develop a Finite Element Model to predict the performance of separator tank pressure vessels used in screw compressor systems subjected to high pressure and temperature and to compare different types of heads manufactured using conventional materials. In addition, after determining the appropriate head type, the separator tank has been numerically modeled using different composite materials and its performance has been examined.

As a result of the study, it has been seen that metal-lined and composite wrapped pressure vessels are safer under applied loading conditions than those designed with conventional materials. In addition, it was decided which dish end, material, and direction angle should be designed to use the separator tank within the safety limits.

Keywords: separator tank, dish end, orientation angle, pressure, equivalent stress, total deformation.

ÖZET

VİDALI TİP KOMPRESÖR SİSTEMLERİNDE KULLANILAN YAĞ SEPERATÖR TANKININ TASARIMI VE ANALİZİ

Volkan GEZGİNCİ
Makine Mühendisliği Anabilim Dalı
Danışman: Dr. Öğr. Üyesi Cem BOĞA
Ocak 2022, 73 sayfa

Basınçlı kaplar tüm kompresör sistemlerinde kilit bir role sahip olan, 0.5 bar'dan daha büyük iç basınca sahip, çeşitli sıvıların depolanması ve taşınması için kullanılan, geometrik olarak silindirik, küresel veya konik iş ekipmanıdır. Basınçlı kaplar, uygun şekilde tasarlanıp imal edilmezlerse veya çalışma koşulları nedeniyle yanlış kullanılırlarsa oluşabilecek hasarlar çevreye ve çalışanlara ciddi zararlar verebilir. Bu çalışmanın odak noktası, yüksek basınç ve sıcaklığa maruz kalan vidalı kompresör sistemlerinde kullanılan seperatör tankı basınçlı kabının performansını tahmin etmek ve geleneksel malzemeler kullanılarak üretilen farklı başlık tiplerini karşılaştırmak için Sonlu Eleman Modeli geliştirmektir. Ayrıca, uygun başlık tipinin belirlenmesinden sonra separator tankı farklı kompozit malzemeler kullanalarak numerik olarak modellenmiş ve performansı incelenmiştir.

Çalışmanın sonucunda, uygulanan yükleme koşulları altında metal astarlı ve kompozit sargılı basınçlı kapların geleneksel malzemelerle tasarlananlara göre daha güvenli olduğu görülmüştür. Ayrıca, seperatör tankının güvenlik limitleri dahilinde kullanılabilmesi için hangi başlık tipi, malzeme ve yönlendirme açısında tasarlanması gerektiğine karar verilmiştir.

Anahtar Kelimeler: separatör tankı, başlık tipi, yönlendirme açısı, basınç, eşdeğer gerilme, birinci kat göçme kriteri, toplam deformasyon.

Dedicated to my beloved wife and children, to my supervisor Asst. Prof. Dr. Cem BOĞA, who did not spare his support during the graduate program, and finally to the chairman of the board of directors of SARMAK, Mr. Murat SARAÇOĞLU.

ACKNOWLEDGEMENTS

First of all, I would like to thank my supervisor Asst. Prof. Dr. Cem BOĞA, for his guiding and positive attitude that encourages me and his vast knowledge that helps me look from different aspects during the study of this master's thesis. I am pleased to say that it was an honor to work with him and be his student.

I would also like to thank Murat SARAÇOĞLU, the chairman of the board of directors of SARMAK, of which I am proud and happy to be a member, for being a source of motivation in the selection of the thesis topic, supporting me and sharing all his knowledge and experience with me.

Last but not least, I would like to express my gratitude and thank my dear wife, Bircan GEZGİNCİ, who was always by my side and supported the decisions I made. Furthermore, I would like to thank Can ÇALIŞKANYÜREK, whom I always received his supports during the thesis writing phase.

TABLE OF CONTENTS

LIST OF FIGURES

LIST OF TABLES

NOMENCLATURE

CAGI	: Compressed Air&Gas Institute
ISO	: International Organization for Standardization
ASME	: American Society of Mechanical Engineer
AD	: Arbeitsgemeinschaft Druckbehaelter
LPG	: Liquid Pressure Gas
S	: Strength
E	: Electrical
PAN	: Polyacrylonitrile
EN	: European
FEA	: Finite Element Analysis
FEM	: Finite Element Method
P265GH	: Heat-resistant pressure-vessel steels
CAD	: Computer-aided design
FPF	: First Ply Failure

1. INTRODUCTION

1.1 Compressor

Compressors are devices that increase the pressure of a gas by reducing its volume. There are two types of the compressors, while one of them is called positive displacement compressors, the other one is called as dynamic compressors (Figure 1.1).

A positive displacement compressor compresses the air by the displacement of a mechanical linkage reducing the volume. Positive displacement compressors can be divided into two different mechanisms. One of its mechanisms is reciprocating compressors, which are used to deliver high-pressure gas using pistons driven by a crankshaft. Diaphragm, double-acting, and single-acting compressors are reciprocating compressors. The diaphragm compressor is a variation of the standard reciprocating compressor. Compression of the gas occurs by the action of a flexible membrane instead of an inlet element. The reciprocating motion of the membrane is driven by a rod and a crankshaft mechanism [38].

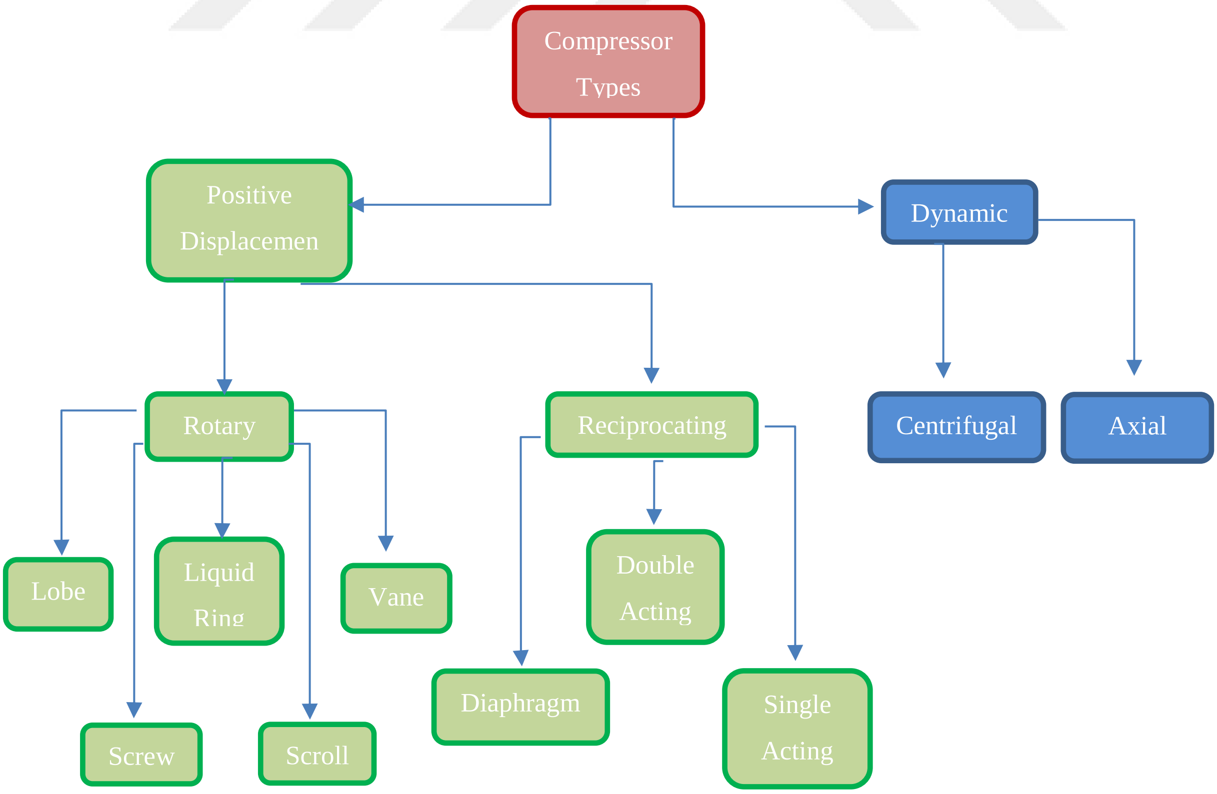

Figure 1.1. Compressor Types

Another mechanism of the positive displacement compressors is rotary compressors. There are five types of rotary compressors: scroll, vane, lobe, liquid ring, and screw. Rotary screw compressors use two braided rotating positive-displacement helical screws to force gas into a smaller space. Screw compressors have fewer moving components, larger capacity, less vibration, and fluctuation, can operate at variable speeds, and typically have higher efficiency. Rotary vane compressors consist of a rotor with several blades placed in radial slots in the rotor. In rotary vane compressors, a series of increasing and decreasing volumes are created by the rotating blades. Another example of rotary compressors is scroll compressors. Also known as a scroll pump and a scroll vacuum pump, a scroll compressor uses two nested spiral-like blades to pump or compress liquids such as liquids and gases. Scroll compressors are more reliable because they have fewer components and simpler construction than reciprocating and rotary reciprocating compressors, they are more efficient because they have no cavity volume and valves, fewer oscillations, and do not vibrate too much. But compared with screw and centrifugal compressors, scroll compressors have lower efficiency and smaller capacity.

The second important compressor type is dynamic compressors. Axial and centrifugal compressors are examples of dynamic compressors. Centrifugal compressors use a rotating disc or impeller in a shaped enclosure to force gas near the impeller and increase the velocity of the gas, while axial compressors are dynamically rotating compressors that use fan-like arrays of blades to gradually compress a liquid [38].

Consequently, compared to the rotary screw compressors, higher pressure gases can be acquired by reciprocating compressors, however, in terms of the continuity and efficiency rotary screw compressors are better options.

1.1.1 History of Rotary Screw Compressors

Heinrich Krigar was living in Hannover, and his design drawings were showing two rotors that have identically the same profiles. Although Krigar's design resembled the root blower rotors that were first come up in Europe in 1867, there was an important difference. In Krigar's design, it was doing winding along the lengths of the lobes and grooves of the rotors with 180 degree. Due to the inadequacy of the production technology, it was not possible to think or develop any further at that time. After a half-century, Swedish steam turbine manufacturer Ljungstroms Angturbin and Alf Lysholm, head engineer of AB company, made very important contributions to the improvement of modern rotary screw compressor.

At those times, Lysholm was researching light compressors to be used in gas and steam turbines. When it coincides with the expiry of the original patent rights, Lysholm tried different rotor combinations. Not only the shape of rotors was important, but there was also the problem of precision machining of rotors, and Lysholm got a patent about the machining of rotors by solving that problem. The patent in 1935 clearly shows that rotors with an asymmetric profile that use five grooves in female rotor counterpart to the four lobs of the male rotor mean the birth of today's rotary screw compressors. This first asymmetrical profiled four-by-five lobed design has been used just the same for years.

1.1.2 Oil-injected Rotary Screw Compressors

In an oil-injected rotary screw compressor, oil is injected into the compression gaps to aid impermeability and to provide cooling for the gas load. The oil leaves the drain stream, is first cooled, then filtered, and finally recycled. The oil effectively reduces the particle load of the compressed air particle filtration by catching the nonpolar particles from incoming air. Usually, some drifting compressor oil moved into a compressed air stream that is downstream of the compressor. In many applications, this problem is fixed via coalescer/filter vessels.

Oil-injected rotary screw compressors are the most common model used in almost all industries. In the latter decade, there are plenty of research conducted to enhance the energy efficiency of compressors and compressed air systems. Compressed air and gas committees; Compressed Air&Gas Institute (CAGI) and Pneurop are making new regulations to increase the energy efficiency of compressors and compressed air systems.

Life cycle costs of compressors are generally calculated for ten years of usage. Although compressors are usually seen as expensive machines while making the first investment, the investment cost is usually around 10-15% of the total cost in ten years.

1.1.2.1 Working Priciple of Oil-injected Rotary Screw Compressors

Oil-injected rotary screw compressors run with the principle of increasing pressure by reducing the volume of a closed chamber. Rotary screw compressor has various parts and systems inside of it. Figure 1.2 shown below is the arrangement of a fundamental rotary screw compressor.

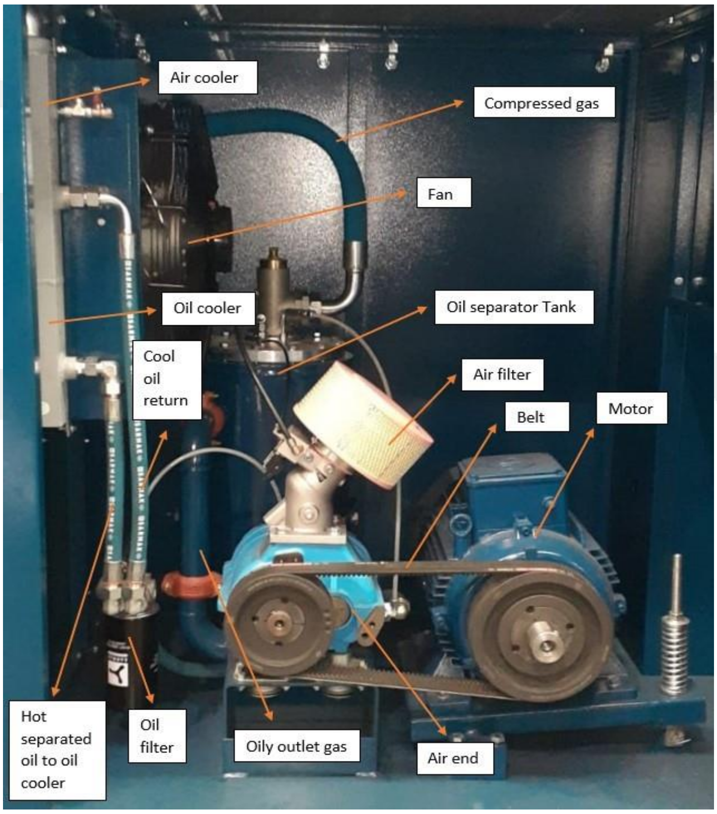

Figure 1.2. Schematic view of a fundamental rotary screw.

There are five systems in an oil-injected rotary screw compressor, namely, drive system, separation system, cooling system, intake control system, and hydraulic system. Since the drive system performs the compression process, it is the most necessary part of the compressor. Belt-pulley or an elastic connection transmits the mechanical energy provided by an electrical motor to the compression element (air end). Figure 1.3 shown below is the cutaway view of the air end.

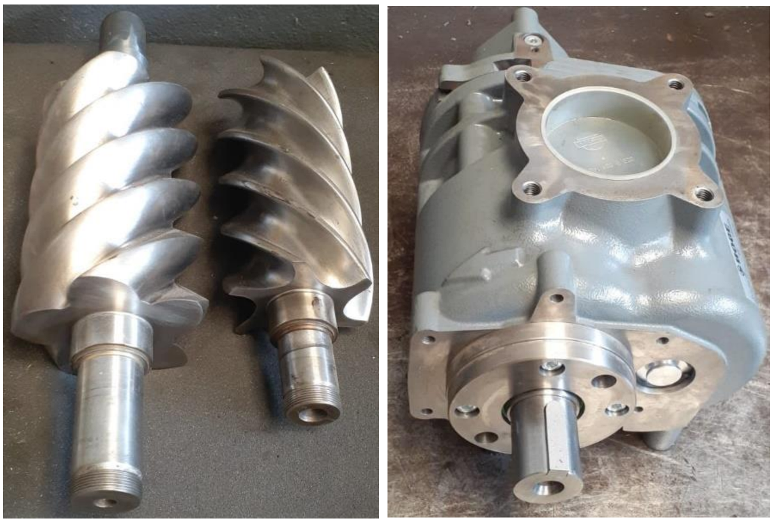

Figure 1.3. Cross-section view of the air end.

The air end (or rotary screw) is the most important unit that the screw compressors are named after. The air end consists of male and female rotors placed into a body. Its complementary elements are caps and bearings. Friction ratios between rotors and their bodies are adjusted very precisely in screws produced with special engineering and fine workmanship. A screw's body is produced generally from casting material, while rotors are produced generally from steel material. The compression operation of screw compressors happens in the body of the airend. The female rotor provides impermeability of the working space during suction and compression phases, while the compressor's motor drives the male rotor directly or via a belt-pulley system. When the compressor is run, the screw unit presses the air, sucked from the upper part of the body, from the lower part with oil. Thanks to the low-pressure valve, the rotating screw first increases the pressure by 1-2 bar and makes the oil in the system circulate. By continuously spraying oil to the screw, protection against the heat is provided, and compressing the air fills the gaps inside of the screw.

1.2 Pressure Vessels

The tanks and storages which are closed structured and have fluid-impermeability are called pressure vessels. A pressure vessel can be defined as a vessel that has pressure differences inside and outside of it. According to the Turkish Standards Institution, to say that a vessel is a pressure vessel, it must be durable for storing and carrying at the pressure level of 0.5 bar. The experimental and numerical studies are carried out with care since it can cause big problems with explosions in case of not paying attention during the production of pressure vessels. Even though they seem simple by appearance, they differ according to their use of areas in terms of design. This difference causes some difficulties with both production and installation in the system. Since variety will affect international usage, some designing standards have been determined by establishments such as the International Organization for Standardization (ISO), American Society of Mechanical Engineers (ASME), and Arbeitsgemeinschaft Druckbehaelter (AD) Merkblatter. Figure 1.4 shown below is the pressure vessel of composite.

Figure 1.4. Composite pressure vessels [42].

Pressure vessels were produced using metal alloys, but since the need for more durable and lighter tanks could not be met with current production methods, manufacturers started to produce pressure vessels using composite materials with the developing technology. After the usage of composites, the fabrication of cylindrical structured pressure vessels began with the fiber winding process. However, these productions were being done depending on the experimental results, but this was not efficient for large pressure vessels. As pressure vessels, hydrophores, heating boilers, steam boilers, autoclaves, compressors, separator tanks, air tanks, industrial gas tanks, cryogenic tanks, LPG tanks, hydraulic and pneumatic fluid circuits, portable gas cylinders (welded, seamless), cooling units, and pressurized pipelines, widely used in industry.

1.2.1 Separator Tank

The separator tank is one of the main items used in screw air compressors. The job of the separator tank is to separate the air circulating with the oil in the screw compressors' system from each other. A special fiber/epoxy filter is being used in the structure of separators. Figure 1.5 shown below is the separator tank.

Figure 1.5. Seperator tank [42].

The air that the screw sucked from outside and the oil inside of the system are sent together to the separator tank. Here, thanks to the separator's filter, oil is kept in the compressor, and from a distinct section to the installation, the separated air is sent.

Separator tanks have the potential to explode, resulting in harm to the environment and people. For this reason, it should be resistant to stresses that may occur at high pressure and temperature. In addition, the lightness of the system in which separator tanks are used will reduce the load and stresses on the mounted chassis. It is aimed to prevent these problems that may be encountered by using composite materials in the analyzed separator tank.

1.3 Composite Materials

A new material formed by a heterogeneous mixture of two or more materials at the micro or macro level to reveal a new material is called composite material. Composite materials have many advantages such as high strength, lightness, flexibility in design, stiffness, wear resistance, high temperature-capacity, aesthetics in material and cost.

1.4 Reinforcement Materials (Fibers/Epoxies)

Fibers/epoxies used in composite materials have so much effect on the characteristics of the physically produced new material. Fundamentally, reinforcement materials consist of three distinct groups: particulate, continuous, and noncontinuous fibers/epoxies. Although the particles generally do not have a spherical structure, they approximately have equal sizes everywhere. Gravels, micro-level balloons, and resin powder particles can be shown as instances of the reinforcement materials. When the reinforcement materials are examined, one size is larger than the others. The measures of short (discontinuous) fibers/epoxies range from millimeter to centimeter. When the diameters of the fibers are examined, it is seen that they do not exceed micrometers. Depending on that, the fiber/epoxy does not necessarily have much length to become fiber from the particulate form. Long (continuous) fibers/epoxies are being used by forming them into string shapes without cutting, using methods like the wire winding method. The fibers/epoxies show their characteristic of having high mechanical strength on their heights compared to their widths. Those characteristics generate extremely anisotropic material features due to the change of direction of the attribute that composite materials have. Therefore, it is necessary to take combinations of fibers/epoxies with resin and their geometric shape into account during the production. It is possible to provide a high advantage by using the anisotropic material feature suitable for the material substitute during the production.

Fibers/epoxies are weaved as fabric to increase the robustness of the material, and to provide the same resistance in all directions. There are types of fiber/epoxy fabrics produced as continuous fibers have types developed for various purposes. The most used reinforcement materials in the industry are glass fiber/epoxy, kevlar fiber/epoxy, and carbon fiber/epoxy.

1.4.1 Glass Fibers/Epoxies

Glass fibers/epoxies occur by pulling through the small hole hives at a certain speed by melting the raw materials that make it up in an oven at approximately 1370-1650 °C. It can be obtained by cooling shortly after it is pulled and by winding on reels. The pulling speed reduces the thickness of the fiber/epoxy.

Figure 1.6. Glass Fiber/Epoxy [35].

Two types of fibers/epoxies, S-glass and E-glass are the most used in the market. S-glass is silica-based and has higher strength and fatigue resistance at higher temperatures. E-glass is boric acid based and has high electrical insulation. The endurance of the S-glass is higher than the E-glass, and the S-glass contains magnesium and aluminum-oxide. Besides its high cost, S-glass is used in places that have high temperature and high tensile strength.

1.4.2 Carbon Fibers/Epoxies

The carbon fibers/epoxies are produced from organic raw materials called PAN (polyacrylonitrile), rayon (cellulose), and pitch. These organic substances become carbonized by oxidation by exposure to high temperatures.

Figure 1.7. Carbon Fiber/Epoxy [36].

PAN-based carbon fiber/epoxy is the most used in the market. Fiber/epoxy matrices are generally used in carbon fibers and combining them shows an extraordinary property in strength and rigidity. While the advantages of carbon fibers/epoxies are high strength, high modulus of elasticity, good fatigue resistance, high thermal temperature, and high electromagnetic interaction compared to other fiber/epoxy types, the disadvantages are high cost and brittleness. The usage areas of carbon fibers/epoxies are; spacecraft, aircraft, sports equipment, turbines, etc.

1.4.3 Kevlar Fibers/Epoxies

Kevlar fibers/epoxies are organic (polymer) based, and these fibers/epoxies contain a propylene polycondensation terephthalatol chloride and p-phenylenediamine. The modulus of elasticity of kevlar fibers/epoxies is lower than carbon fibers/epoxies but higher than glass fibers/epoxies. Besides, kevlar fibers/epoxies have high strength, low density, high chemical resistance, and high fatigue endurance compared to carbon-glass fibers/epoxies. The disadvantage of kevlar fibers/epoxies is that kevlar fibers/epoxies combine with matrix material less than other fibers/epoxies. For this reason, small cracks occur in the resins. Due to its sensitivity to water, the rate of humidity increases, and its cost is higher than the glass and carbon fibers/epoxies. The usage areas of kevlar fibers/epoxies are defense industry, bulletproof vests, boat hulls, ballistic applications, etc.

Figure 1.8. Kevlar Fiber/epoxy [37].

1.5 Application Areas of Composite Materials

Composites are used increasingly in industry and technology applications with the advances in composite material technology. Scientific studies on composites, which are used significantly in the aircraft industry and many other sectors, continue intensively today. Composite materials are used in a wide variety of fields thanks to their structure and properties. Since each sector has different needs and expectations, the product flexibility of composite materials is an important advantage. Composites are used as raw materials in different sectors as well as manufacturing auxiliary equipment. The main sectors where composite materials are widely used and the product types used in these sectors can be summarized under the headings as space technology, maritime industry, medical device manufacturing, robot technology, chemical industry, electrical-electronic technology, musical instruments industry, construction and building industry, automotive industry, defense industry and aviation sector, food and agriculture sector, sports equipment manufacturing [1].

2. LITERATURE REVIEW

In the previous section, information was given about the classification, history, components, and operating principles of compressors. Additionally, an explanation was made about the definition and application areas of pressure vessels, which are components of the compressor system. In this section, information from different theses and articles is presented to support the study.

Bozkurt [1] has designed the vessels using filament and centrifugal winding methods, composite materials (glass fiber/epoxy, carbon fiber/epoxy, and kevlar fiber/epoxy), and antisymmetric orientation angles ([30°/-30°], [45°/-45°], [60°/-60°] ve [75°/-75°]). He used the finite element approach to analyze the maximal strain and stresses with the ANSYS WORKBENCH 14.0 package application. By examining the Von-Mises stresses and total deformations obtained in the solutions, Bozkurt has determined that the optimum value of the maximum stresses occurs in pressure vessels designed with glass fiber/epoxy composite material with an orientation angle of 60°/-60°, and the optimum value of the strain occurred in carbon fiber/epoxy composite pressure vessels with an orientation angle of 60°/-60°.

Sancaklı [2] gave the basic design rules of pressure vessels according to the codes of ASME Section 8 Part 1, ASME Section 8 Part 2, EN 13445, and AD 2000. Then, with an exemplary application, made calculations of an air tank with certain design conditions and geometric features according to 4 codes, found the minimum wall thicknesses according to three different head types (elliptical, torispheric, and hemispherical), and calculated the weights according to these thicknesses. Thus, he has aimed to provide benefits to engineers and researchers working in this field in the selection of the appropriate code for pressure vessel design and the design of the lowest-cost vessel with desired features.

Balcı [3] has developed a decision support system called MATSEL, which consists of two parts and can choose the most appropriate material according to the working environment of the pressure vessel part. The first stage of the MATSEL program was the pre-elimination process, and material alternatives were screened into suitable candidate materials with variable questions and limit values. In the next stage of the MATSEL program, appropriate decision sequences were created with the multi-criteria decision-making methods TOPSIS, ELEKTRE, and VIKOR. He has created the material properties in the database by taking data from ASME, BPVC, and CES software and explained the usage of the MATSEL program and how it was formed within the scope of the thesis. The obtained results were subjected to Spearman Ranks Correlation, and the fit rates were calculated.

Mestan [4] examined the experimental results by applying hydrostatic pressure tests to the pressure vessels under the influence of internal pressure. Pressure vessels contain potential hazards that will affect human health and safety. For this reason, a careful and detailed analysis should be made in pressure vessel design, and all loads that may affect the system should be accurately determined and included in the calculations. Mestan has compared the theoretical approximation solution of a cylindrical pressure vessel subjected to axially symmetrical loading and the displacement and stresses obtained as a result of Von Mises stress analysis from the SOLIDWORKS program. While analyzing, the "COSMOSXpress Analysis Wizard" computer program, which uses the finite element method was used.

Usta [5] aimed to investigate whether welded joints (area under heat effect) made in the design and production of thick-walled pressure vessels can withstand the pressures determined according to TS 377 standard. As a result of the hydrostatic tests carried out in pressure vessels, the welded areas of the heating boiler, steam boiler, and air tank were inspected according to TS 17020 standard. When high pressure is applied to the thick-walled pressurized vessel, Usta has determined whether the region under the effect of heat can provide the required strength values, its suitability for dynamic working conditions, and the formation of perspiration, leakage, or cracks at the welding points. It was observed that the welded areas of pressure vessels are appropriate.

Kandaz [6] aimed to design and analyze the pressure vessel and related pressure equipment with various standards and methods. As the main output of the study, Kandaz has developed a computer program that can make rapid and comprehensive analyses with the mentioned methods. Also examined the effects of wind, earthquake, and other loading types in detail with dynamic analysis. He developed a computer program named VESSELAID in SI units using Microsoft Visual Basic 6.0. VESSELAID's design and analysis methods were based on the rules introduced by various standards, frequently used and recommended design methods, and different approaches.

Yıldırım [7] developed pressure cells in a thin-walled aluminum tube and increased strength by injecting compressed air of varying pressures into these cells. When looking at the graphical results of the three-point bending and compression test obtained from experimental studies, Yıldırım observed that the maximum load the aluminum tube can carry when subjected to a dynamic load under 30 psi internal pressure is 4.5 times greater than the maximum load it could carry when there is no internal pressure (0 psi). Yıldırım compared both analytical and numerical calculation results of X-direction stress, Y-direction stress, and Von Misses stresses under 0.723 MPa (105 psi) internal pressure in aluminum tube and obtained very close values.

Tjelta [8] investigated and explained the advantages and disadvantages of the different methods used for pressure vessel design. Tjelta presented some theory and examples to give a general understanding of the elastic-plastic method, established a complete design basis including the complete construction drawing sets, part lists, 3D models, and material properties for a heavy wall pressure vessel and a thin wall pressure vessel, described the tools used in the analysis in detail, and carried out the calculation for the relevant standard and presented the approach and the results in table format for easy comparison.

Raparla and Seshaiah [9] examined the advantages of multilayer high-pressure vessels according to the ASME VIII-1 standard over single-layer high-pressure vessels. They compared the theoretically calculated results of the stresses in the vessel with the results obtained from Ansys program. It has detected that the multi-layer designed vessel cost 26% less than the single layer, that the strain variation along the thickness was less, and that it was more advantageous at high temperature and pressure.

Ahmed et al. [10] calculated the Von-Mises stresses, tangential stresses, and deformations in pressure vessels with different geometries subjected to thermal and static loads using the finite element method (ANSYS) for optimization. As a result, they have found that tangential stresses will increase with the decrease in pressure vessel thickness.

Yaylağan [11] has investigated the optimal layer-angle orientation of antisymmetric stratified, thin-walled, internally plastic-liner composite pressure tubes for first layer damage at different temperatures and maximum blast pressure by doing finite element method and experimental studies. As a result, he has found that the most suitable winding angle in composite tubes with helical angle winding under internal pressure was around 55º.

Baba [12] theoretically examined the distribution of stress in Laplace space, the anisotropic material made of special-orthotropic material thick-wall hollow cylinders and spherical pressure vessels. By applying various axial symmetrical dynamic pressures to the inner surface, he has determined tangential stresses by radial displacement.

Wadkar et al. [13] designed various pressure vessels with different types of heads (ellipsoidal, hemispherical, torispheric, conical, iconic, and straight) according to ASME VIII-1 and analytically calculated and compared with equivalent numerical stresses (ANSYS). After observing that the results are in harmony, they have observed the smallest equivalent stresses in the hemispherical-headed cylindrical vessel.

Kolekar and Jewargi [14] have analyzed the pressure vessel with 8 bar pressure and 24-liter volume designed according to ASME VIII-1 in five different head types (hemispherical, flanged, elliptical, flat, and conical) using the ANSYS program. As a result, they have observed that the least stress occurred in the hemispherical head. However, due to the material costs and the industry's demand for optimization, they discovered that it was reasonable to select the elliptical head in the safe zone.

Pehlivan [15] worked on the modeling of composite pressure vessels produced with fiber winding production techniques at different loads. Analytical and numerical (ANSYS) results after verifying each other by evaluating the compressive strength, he determined the optimum angle values of the structure.

Poojary et al. [16] wanted to determine the reliability of the flat head pressure vessel, made of Tu 283 C, by determining Von-Mises stresses under a certain pressure (10.3421 bar). They have used the ANSYS program in their studies. As a result, the maximum stresses obtained have proved that the pressure vessel material is lower than the yield stress, therefore the pressure vessel is safe.

Sinha and Pandit [17] conducted a study on the cylindrical portion of a four-layer carbon fiber reinforced polymer composite (CFRP) pressure vessel. The pressure vessel was designed and modeled using the finite element software ANSYS 11. They estimated burst pressures for various fiber orientations using Tsai-Wu criteria. As a result, they have obtained the fiber orientation angle of ± 45° as the optimum fiber orientation angle for the composite pressure vessel subjected to high internal pressure load.

Kadam et al. [18] conducted finite element analyses (FEA) to predict the element analysis of static burst pressure in close thick-walled irregular cylinders and compared the result with the Svensson burst model. Cylinders that are thick-walled and have different diameter ratios have been examined. As a result, using finite element analysis (FEA) has proved that predicted static burst pressure is compatible with the Svensson model.

Li et al. [19] by using the finite element method (FEM) model, focused on a formula that is intended for the suppression of the pressure while the ellipsoidal head was under inner pressure. In addition, in buckling pressure of the ellipsoidal heads, has investigated diameter-thickness ratio, radius-height ratio, yield strength, and effect of tensile stiffness. As a result, it was observed that the presciences of the acquired new formula were reasonably compatible with the experimental results.

Khan et al. [20] examined the effect of the load applied on the support legs of the pressure vessel by changing various geometrical parameters. They have aimed to give suggestions related to the optimal values, which are supposed to be, the ratio of the support distance to the pressure vessel's length and the ratio of the pressure vessel's length to the vessel's radius. Consequently, they have determined that for the ratio of the support distance to the length of the pressure vessel, minimum stresses occurred valued at 0.25, and in case of the ratio of the length of the pressure vessel to the vessel's radius being less than 16, minimum stresses occurred on the pressure vessel and the legs.

Carborani et al. [21] of the whole pressure vessel model aiming to minimize the mechanical stress from nozzle to the head, have researched the shape optimization of the axial symmetrical pressure vessels. Taking the temperature and pressure load into account they have acquired solutions for the entire pressure vessel. The work done by acquiring different shapes other than the usual ones has been remarkable. According to the work done by using ANSYS – APDL, they have determined that surfaces that are not sharp transitional have less stress than the sharp transitional surfaces. The pressure vessel consists of 3 parts (head, nozzle, and body). They have also determined that considering thermal loads, stresses of the body and nozzle are being close to each other, but, when there is no thermal load, stress on the body (cylinder) is higher from the stresses that occurred on the head and nozzles.

Zhang et al. [22] based on the theory of thermo-elasticity, have acquired an analytic solution to determine the stress distribution of a multi-layered composite pressure vessel exposed to inner fluid pressure and a thermal load. They have verified the acquired result via FE analysis. As a result, they have determined that the suggested process, can be used at the first stage of designing a multi-layered composite pressure vessel containing fluid pressure and thermal load.

Al-Gathani et al. [23] presented the findings, acquired via the finite element study, of the effect of the pressure vessel’s head size on the stresses close to the junction points where a cylindrical nozzle under inner pressure joins with a spherical vessel. Consequently, they have shown that the required minimum head size is linearly related to the nozzle size, however, its value is generally bigger. they have concluded that a safe local pressure test should relatively use big head sizes and that adequately sized heads smaller than the nozzle may not be acceptable.

Şenalp [24] examined the effects of four different perturbation load models on torispheric heads by using the ANSYS program. Şenalp said that eigenvalue results when compared to the nonlinear solutions and eigenvalue solutions do not provide the same deformation modes. However, he has determined that in nonlinear solutions, points -where maxima occur- show a good match with perturbation mode.

Alcántar et al. [25] explained the optimization of two laminated composites and two Type 4 composite pressure vessel models: genetic algorithm (GA) and simulated annealing (SA). Both approaches have been observed to be similarly successful in producing high-quality optima. They have also observed that SA reaches a better optimum in composite optimization as the presence of many local minimums affects more of the ability of GA to achieve a better optimum, possibly due to the advantage of disrupting existing solutions compared to combining potentially similar individuals.

Joshi and Acharya [26] investigated the effect of seat number, wrap angle, wear plate width, and wear plate elongation on vein and seat stress. Results were obtained from FEA and ANOVA (analysis of variance) of responses (stresses) at various locations. They concluded that the number of saddles affects only the stress distribution in the saddle, but not the stress distribution in pressure vessels.

Kumar et al. [27] proposed the best stiffener design, considering the factors such as specific structural stiffness, von mises stress, weight, and total deformation. They discovered that the spiral stiffener design has 23% less von mises stress than the base roller in terms of strength. However, in terms of stiffness, the spiral reinforcement design produced slightly more deformation than the base roller. Based on these results, the helical stiffener design has been advocated as the optimal design in these reinforcing elements if the deformation is within the limit of applicability.

Alegre et al. [28] through the wire winding technique, evaluated several solutions as follows: changing the winding tension for different layers of winding discontinuously, considering the existing difference between the elastic modulus of the hull and the wound material, etc. They determined the internal collapse pressure to meet the ASME code requirements for such vessels.

Hyder and Asif [29] concluded that the location and size of the hole depend on the size of the cylinder. For a particular application and size of the cylinder, the location and size of the opening should be determined by performing finite element analysis (such as ANSYS), considering the last effects brought by the flanges. The optimum location is where the Von-Mises stress is minimum, and the hole size should be such that the Von Mises stresses are minimal around the perimeter of the hole.

Mehtre [30] showed that the weight of the pressure vessel metallic liner wrapped with composite material is reduced by 25-33% due to the low density of composite material. Mehtre observed that the safety factor in the carbon steel model and the metallic liner wrapped with a composite material remained the same after reducing the total thickness by 10 mm. The operating cost, maintenance cost, and labor cost associated with the operation of the pressure vessel are reduced as the weight of the pressure vessel has reduced by 25-33%, since hot insulation is not required.

Bouvier et al. [31] gave some keys to the appropriate fiber selected for design optimization according to different indicators. These variant indicators that may be the opposite are the mechanical performances, the vessel mass, the vessel cost, and the greenhouse gas emissions. They proved the best fiber-reinforced polymer composite according to the fundamental indicator and for two storage pressures- 700 bar and 350 bar. Other parameters for mechanical performances such as component aging, corrosion, or fire resistance should be considered in material selection.

Siva Kumar et al. [32] carried out the analysis with three different materials on both model parts and compared the results. They observed that the stress and deformation values of the modified model are better than the real model because the lifetime of the vessel may increase due to the decrease in the stress values. They concluded that SA516GR65 can be used for the pressure vessel design and that the life of the pressure vessel can be increased with minor changes in the design.

Akarsu [33] calculated the thermal stresses in composite plates that occurred due to the uniform temperature effect, using the finite element method. The normal thermal stress distributions, shear stresses, co-stress curves occurring in symmetrical and antisymmetric plates with the effect of uniform temperature applied are shown with the help of color contours. After the investigations, seen that the thermal stress values increase depending on the uniform temperature increase applied. This situation is similar for both symmetrical and antisymmetric orientations.

Yıldırım [34] carried out the experimental studies of glass fiber/epoxy and kevlar fiber/epoxy composite materials, and ten separate samples reinforced with the thermoplastic matrix. Using experimental and numerical methods, he investigated the stress state of the composite materials and their effect on mechanical properties. For the determination of mechanical properties, the author examined the shrinkage of the test specimens made of kevlar fiber/epoxy, glass fiber/epoxy, and thermoplastic matrix reinforced composite materials. Yıldırım determined the mechanical properties between these materials, and he observed that the strength of thermoplastic materials improved after being reinforced with fiber.

In this thesis, the separator tank used in SARMAK screw compressor systems and produced according to ISO 1217 standard is discussed. First of all, analyzes were made on the body sheet for three different heads as torispheric, elliptical and flat, and the separator tank operates at three different pressures of 11.25, 15, and 19.5 bar and a maximum temperature of 110 °C. Maximum equivalent stress and maximum total deformation values were calculated separately for two different materials such as P265GH and P235GH. Then, according to the results obtained, the first layer of the separator tank was covered with metal material giving the most suitable stress and deformation values, and the other layers were covered with three different composite materials such as carbon fiber/epoxy, glass fiber/epoxy and kevlar fiber/epoxy at different angles and analyzes were carried out.

3. MATERIALS AND METHODS

In this section, the selected geometries for analysis are presented. Various situations under different head types, materials and pressures are studied. Carbon steel, stainless steel, titanium, and their alloys have traditionally been used to produce pressure vessels. Composite materials are suitable substitutes for these traditionally used materials. To examine the effect of composite material, the following situations are discussed [30]. In this study, the following cases are handled separately, and the total deformation and stress values are examined using the finite element method.

Case 1: 4 mm structure steel.

Case 2: 0.5 mm structure steel covered with 3.5 mm E-glass.

Case 3: 0.5 mm structure steel covered with 3.5 mm E-kevlar.

Case 4: 0.5 mm structure steel covered with 3.5 mm E-carbon.

3.1 Geometry

As can be seen in Figure 3.1, the separator pressure vessel consists of top flange, cylindrical shell, three different dish ends (flat, elliptical, torispheric), and leg support. Figures 3.2, 3.3, and 3.4 show the three different dish ends with geometrical dimensioning.

Figure 3.1. Figure of in-house developed oil separator pressure vessel components.

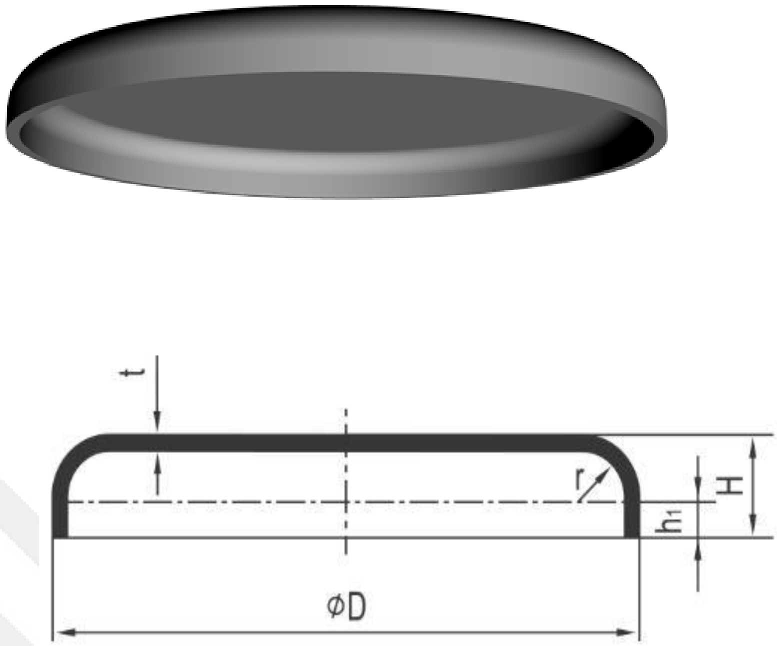

Figure 3.2. Flat dish end geometrical dimensioning.

Technical details for flat dish end [39]:

$$H = h_1 + r + t \tag{1}$$

Where, H is the total height of the dish end, h_1 is the cord height of dish end (between 20 mm –100 mm), radius (r) is between 25 mm – 100 mm, t is the thickness of the dish end, and D is the unit of diameter of the dish end.

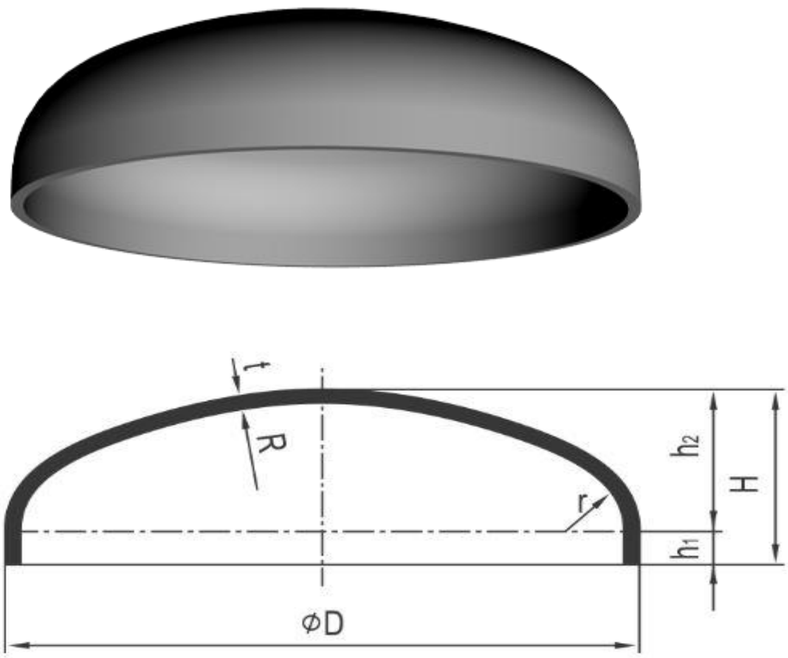

Figure 3.3. Elliptical dish end geometrical dimensioning.

Technical details for elliptical dish end [39]:

$$R = 0.8D \tag{2}$$

$$r = 0.154D \tag{3}$$

$$h_1 \geq 3.5t \tag{4}$$

$$h_2 = 0.26D \tag{5}$$

$$H = h_1 + h_2 \tag{6}$$

Where, h_2 is the height obtained by subtracting the cord height of the dish end h_1 from the height of the dish end H.

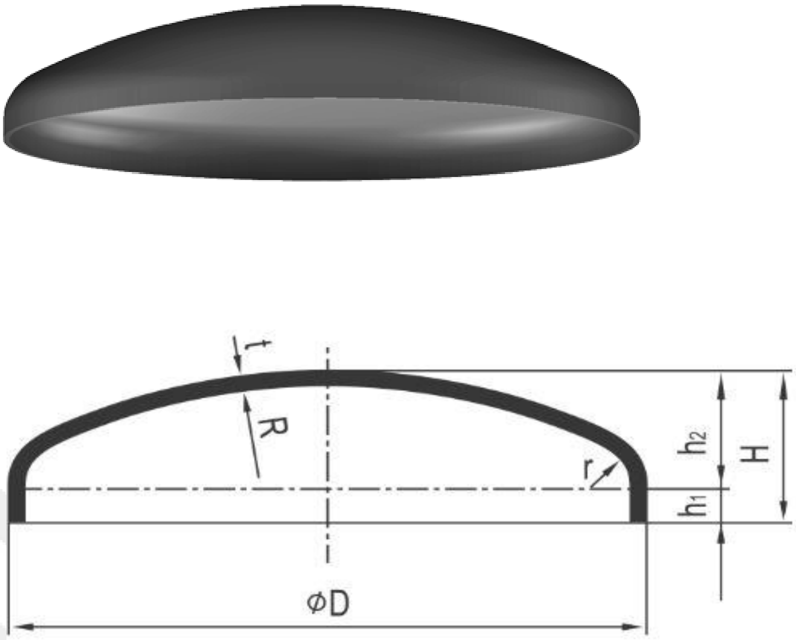

Figure 3.4. Torispheric dish end geometrical dimensioning.

Technical details for torispheric dish end [39]:

$$R = D \tag{7}$$

$$r = 0.1D \tag{8}$$

$$h_1 \geq 3.5t \tag{9}$$

$$h_2 = 0.2D \tag{10}$$

$$H = h_1 + h_2 \tag{11}$$

3.2 Part Design for Separator Vessel with 4 mm Structure Steel

As a solid model, it was designed as a pressure vessel shell model by 29 / EU / 2014 standards designed in the AUTODESK INVERTOR package program. The CAD model of the separator pressure vessel was examined referring to layouts with different dish ends. The total height of the separator pressure vessel from the top flange to the leg support is 698 mm. The thickness of the dish ends, and the cylindrical shell is 4 mm. The thickness of the flange is 24 mm. The inside radius of the separator pressure vessel is 342 mm. The reason for choosing the upper flange thickness to be larger than the thickness of the cylindrical shell is that the stresses on sharp surfaces are higher. Thus, a surface thickness that is more resistant to stresses is preferred in the upper flange with sharp corners.

Figure 3.5, Figure 3.6, and Figure 3.7 show all the important dimensions of separator pressure vessel with flat, elliptical and torispheric dish ends along with all the components.

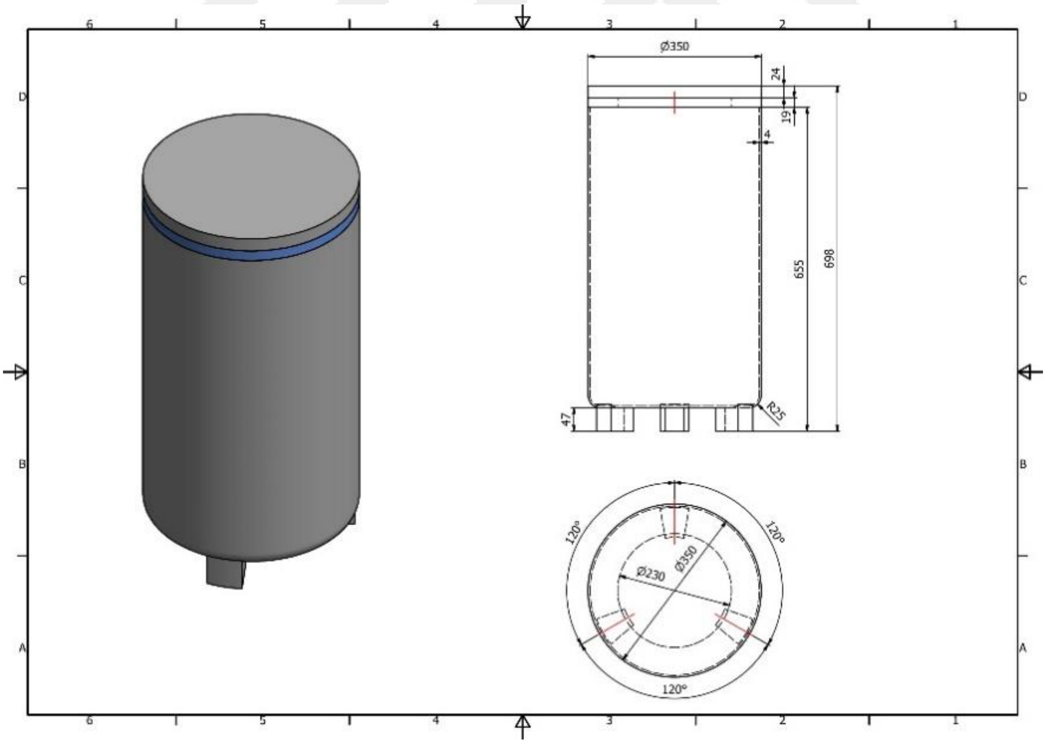

Figure 3.5. Separator vessel with 4 mm structure steel and flat dish end.

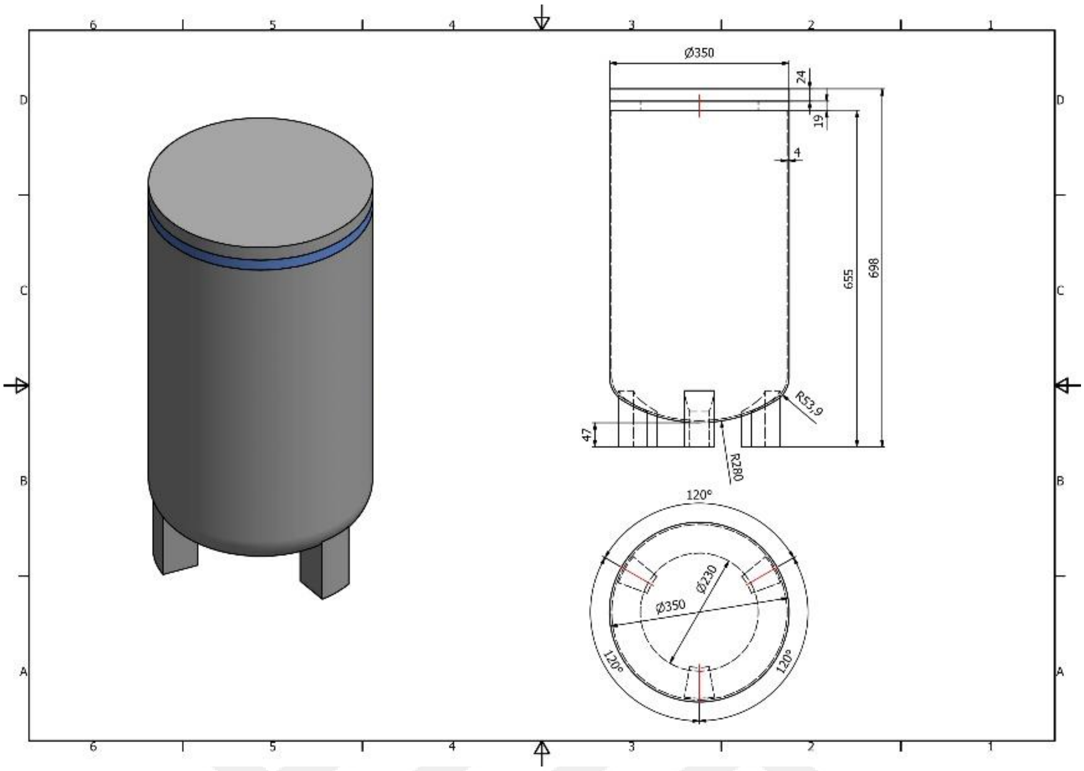

Figure 3.6. Separator vessel with 4 mm structure steel and elliptical dish end.

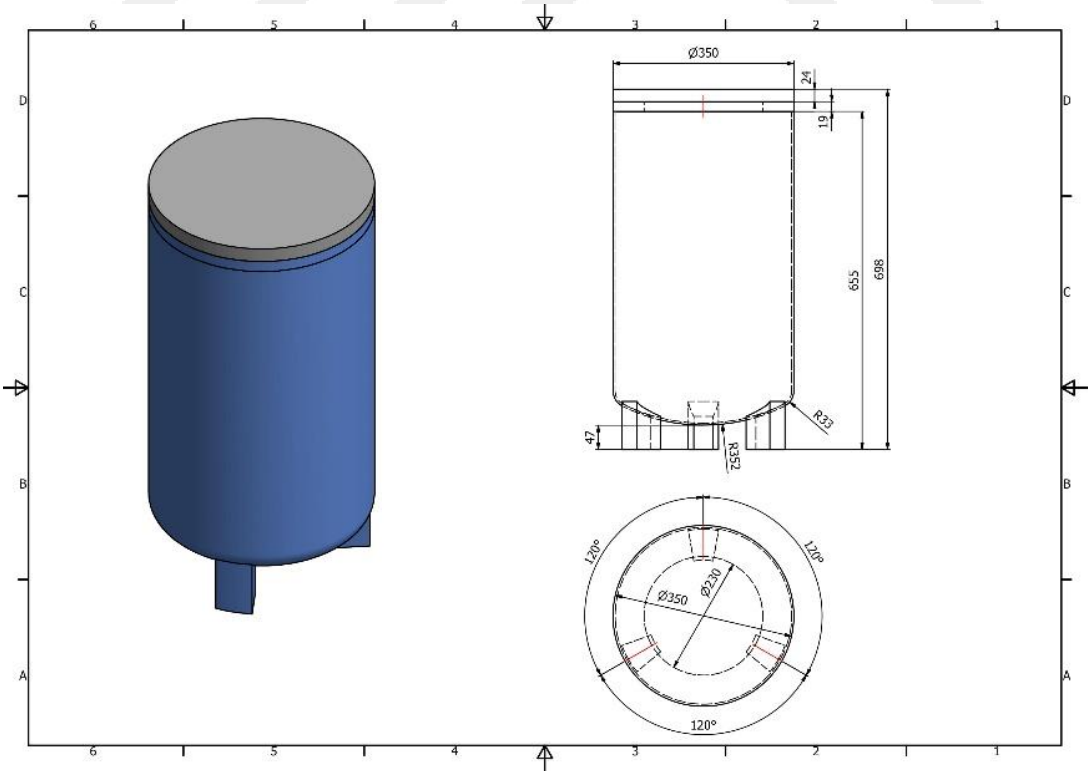

Figure 3.7. Separator vessel with 4 mm structure steel and torispheric dish end.

3.3 Meshing for separator vessel with 4 mm structure steel

The solid model consists of infinitesimal elements, but in analysis with ANSYS, the mesh must be limited to small elements. Because the solver will calculate the points on these finite elements and give results accordingly. In the finite element method program, the mesh size is determined according to various criteria. For example, in ANSYS, the skewness rate is required to be below 0.9 as a criterion. The skewness rate was taken into account when determining the mesh size. Meshing was done using an element sizing tool using tetrahedron and hexahedron elements. Table 3.1 shows number of nodes, and the number of elements for 4 mm structure steels in each case. Figure 3.8 shows meshed CAD models for 4 mm structure steels in each case.

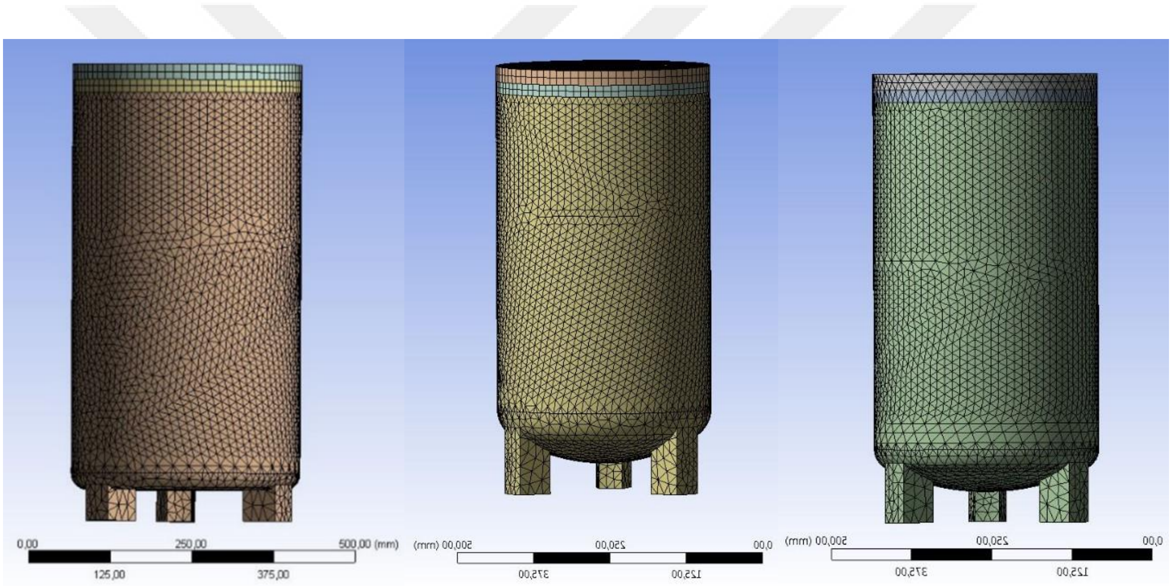

a) Flat Dish End b) Elliptical Dish End c) Torispheric Dish End

Figure 3.8. Meshed CAD Model for 4 mm structure steel.

Table 3.1. Mesh data for 4 mm structure steel.

4 mm structure steel	Number of Nodes	Number of Elements
Flat End	67234	29054
Elliptical End	62898	27205
Torispheric End	52844	26808

3.4 Boundary Conditions

Pressure vessels are subjected to hydrostatic test pressure, depending on this hydrostatic test pressure, our boundary conditions are determined as 1.5 times the operating pressure. Respectively, the boundary condition for 7.5 bar internal pressure is 11.25 bar, the boundary condition for 10 bar internal pressure is 15 bar, and finally, the boundary condition for 13 bar internal pressure is 19.5 bar. Also, constant 110 °C internal temperature and 20 °C ambient temperature are given for each tank. Figure 3.9 given below shows the boundary conditions of the pressure vessel.

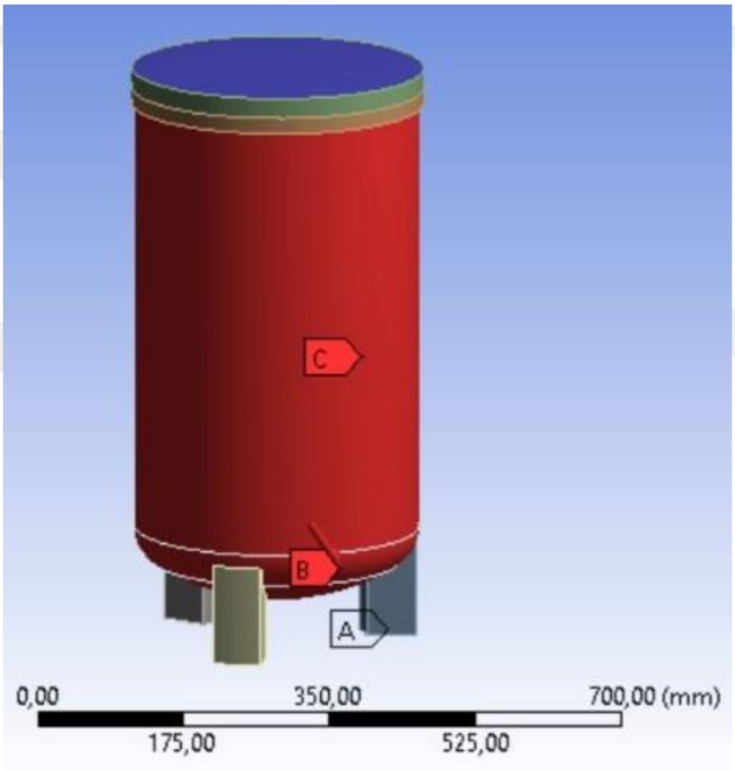

Figure 3.9. Boundary condition.

3.5 Finite Element Analysis

The use of composite materials, which has become widespread recently, has also increased the production of pressure vessels. The filament winding method and centrifuge winding method are used in the production of these composites [11]. The model to be used in the study was compared for three different materials, namely glass fiber/epoxy, carbon fiber/epoxy, and kevlar fiber/epoxy, according to the variable parameters such as different winding angles, different pressure values , and different dish ends. ANSYS analysis program- finite element method- was used while analyzing. The model to be analyzed was designed using AUTODESK INVENTOR, which is a solid model creation program. The models were created after the modeling process was transferred to the ANSYS program and the material properties of the shell model were defined.

The thickness of each layer to be used in the study was accepted as 0.5 mm. For each material, the shape of the bowl ends was modeled to be used as flat, elliptical, or torispheric, and necessary solutions were made. Models were designed with four different winding angles for each layer as [35°/-35°], [45°/-45°], [55°/-55°] or [65°/-65°] and necessary analyzes were made. For each model, the vessel was analyzed with working pressures of 7.5 bar, 10 bar, or 13 bar. The pressure to be applied while making the solutions is defined as 1.5 times the working pressure of the tank and depending on the hydrostatic test pressure. The Von-Mises stresses and total deformations obtained as a result of these solutions were examined and it was determined which design is more applicable.

Carbon, glass, and kevlar fibers/epoxies are used as reinforcements materials. Important properties to be considered for structural and thermal analysis are density, Young’s modulus, Poisson’s ratio, tensile, and shear modulus. The mechanical and thermal properties of carbon, glass, and kevlar fibers/epoxies and structure steel without composites are given in Table 3.2, Table 3.3, Table 3.4, and Table 3.5 [40].

Table 3.2. Properties of 4 mm Structure Steel

Properties	**4 mm Structure Steel**
Density (kg / m^3)	7850
Young's Modulus (MPa)	1.98E+5
Poisson's Ratio	0.35
Tensile Yield Strength (MPa)	265
Shear Modulus (MPa)	73333

Table 3.3. Properties of Carbon Fiber/Epoxy

Properties	**Carbon Fiber/Epoxy**
Density (kg / m^3)	1490
Young's Modulus (MPa) (x, y, z)	1.21E+0.5; 8600; 8600
Poisson's Ratio (xy, yz, xz)	0.27; 0.4; 0.27
Tensile (MPa) (x, y, z)	2231; 29; 29
Shear Modulus (MPa) (xy, yz, xz)	4700; 3100; 4100

Table 3.4. Properties of Glass Fiber/Epoxy

Properties	**Glass Fiber/Epoxy**
Density (kg / m^3)	2000
Young's Modulus (MPa) (x, y, z)	45000; 10000; 10000
Poisson's Ratio (xy, yz, xz)	0.3; 0.4; 0.3
Tensile (MPa) (x, y, z)	1100; 35; 35
Shear Modulus (MPa) (xy, yz, xz)	80; 46.154; 80

Table 3.5. Properties of Kevlar Fiber/Epoxy

Properties	**Kevlar Fiber/Epoxy**
Density (kg / m^3)	1402
Young's Modulus (MPa) (x, y, z)	95710; 1.045E+5; 1.045E+5
Poisson's Ratio (xy, yz, xz)	0.34; 0.37; 0.34
Tensile (MPa) (x, y, z)	2231; 29; 29
Shear Modulus (MPa) (xy, yz, xz)	25080; 25080; 25080

ANSYS package program was used to determine the stress and total deformation. As seen in Figure 3.10 below, ACP (Pre) module to cover the design with composite, Static Structural module to determine boundary conditions and ACP (Result) module to read the results are transferred to the Workbench menu from the Toolbox menu of the program.

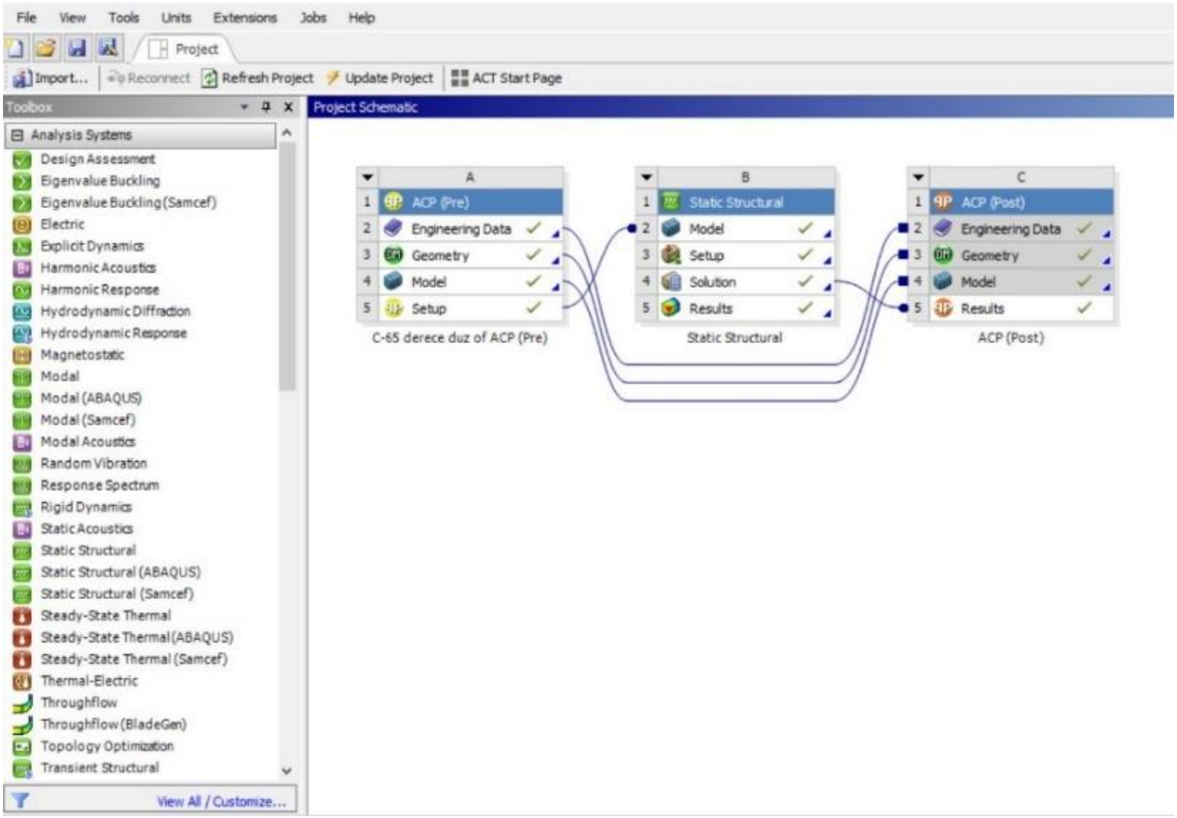

Figure 3.10. Ansys Workbench Interface.

As can be seen in Figure 3.11, the mechanical properties of composite materials used in the study, which are glass fiber/epoxy, carbon fiber/epoxy, and Kevlar fiber/epoxy, are taken from the Engineering Data menu. Since the pressure vessel is designed as layered, taking the properties of the materials is selected from the Toolbox menu according to the Density and Orthotropic Elasticity properties, then Young's Modulus (X ≠Y=Z) MPa, Poisson's Ratio (XY = XZ ≠ YZ) and Shear Modulus (XY = XZ ≠ YZ) MPa the numerical values of the material properties have been taken.

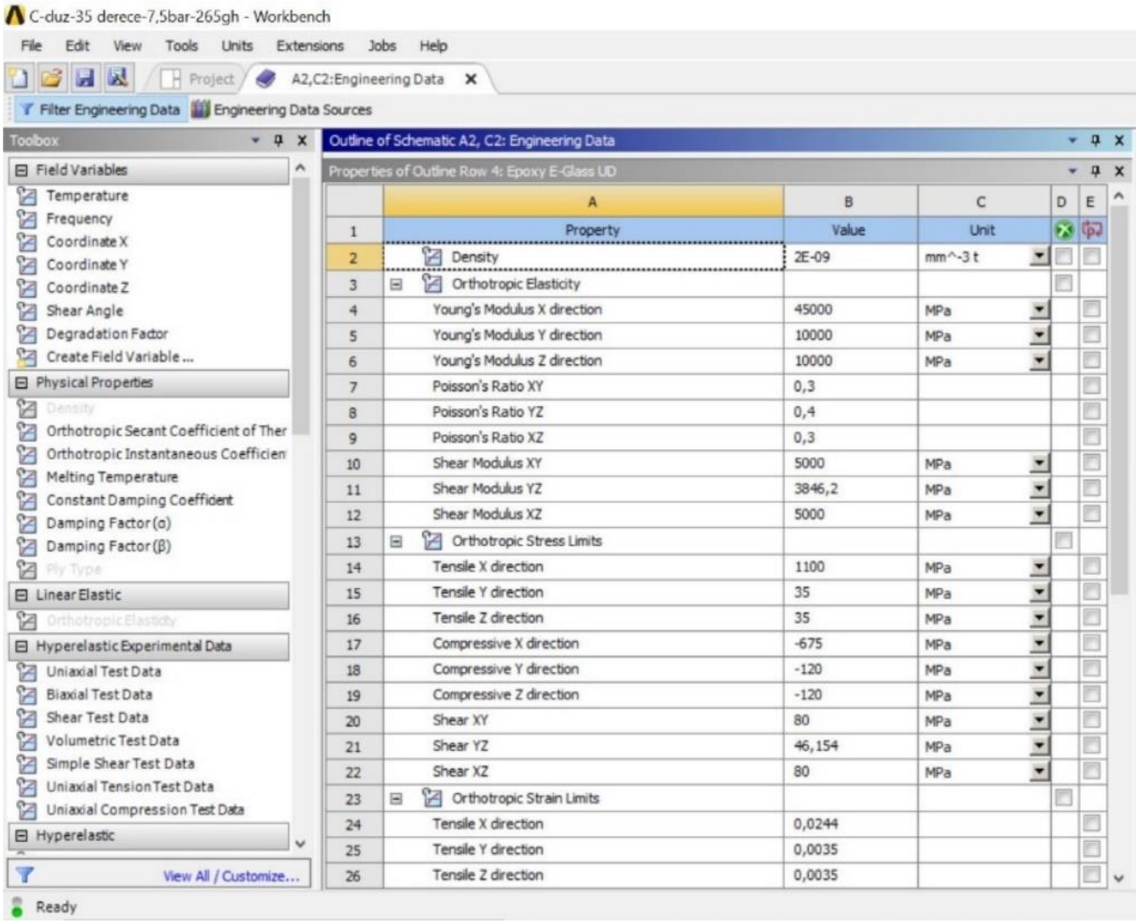

	A	B	C
1	Property	Value	Unit
2	Density	2E-09	mm^-3 t
3	Orthotropic Elasticity		
4	Young's Modulus X direction	45000	MPa
5	Young's Modulus Y direction	10000	MPa
6	Young's Modulus Z direction	10000	MPa
7	Poisson's Ratio XY	0,3	
8	Poisson's Ratio YZ	0,4	
9	Poisson's Ratio XZ	0,3	
10	Shear Modulus XY	5000	MPa
11	Shear Modulus YZ	3846,2	MPa
12	Shear Modulus XZ	5000	MPa
13	Orthotropic Stress Limits		
14	Tensile X direction	1100	MPa
15	Tensile Y direction	35	MPa
16	Tensile Z direction	35	MPa
17	Compressive X direction	-675	MPa
18	Compressive Y direction	-120	MPa
19	Compressive Z direction	-120	MPa
20	Shear XY	80	MPa
21	Shear YZ	46,154	MPa
22	Shear XZ	80	MPa
23	Orthotropic Strain Limits		
24	Tensile X direction	0,0244	
25	Tensile Y direction	0,0035	
26	Tensile Z direction	0,0035	

Figure 3.11. Engineering Data Menu

In the outline menu of the pressure vessel designed in Figure 3.12, the geometry consists of three elements in the Model section. The total layer thickness from the Thickness part of each element and the composite material feature from the assignment part has been selected. In the study, the total layer thickness is 4 mm. After entering the numerical values of the elements, the Layered Section is selected from the Geometry section since the pressure vessel will be layered.

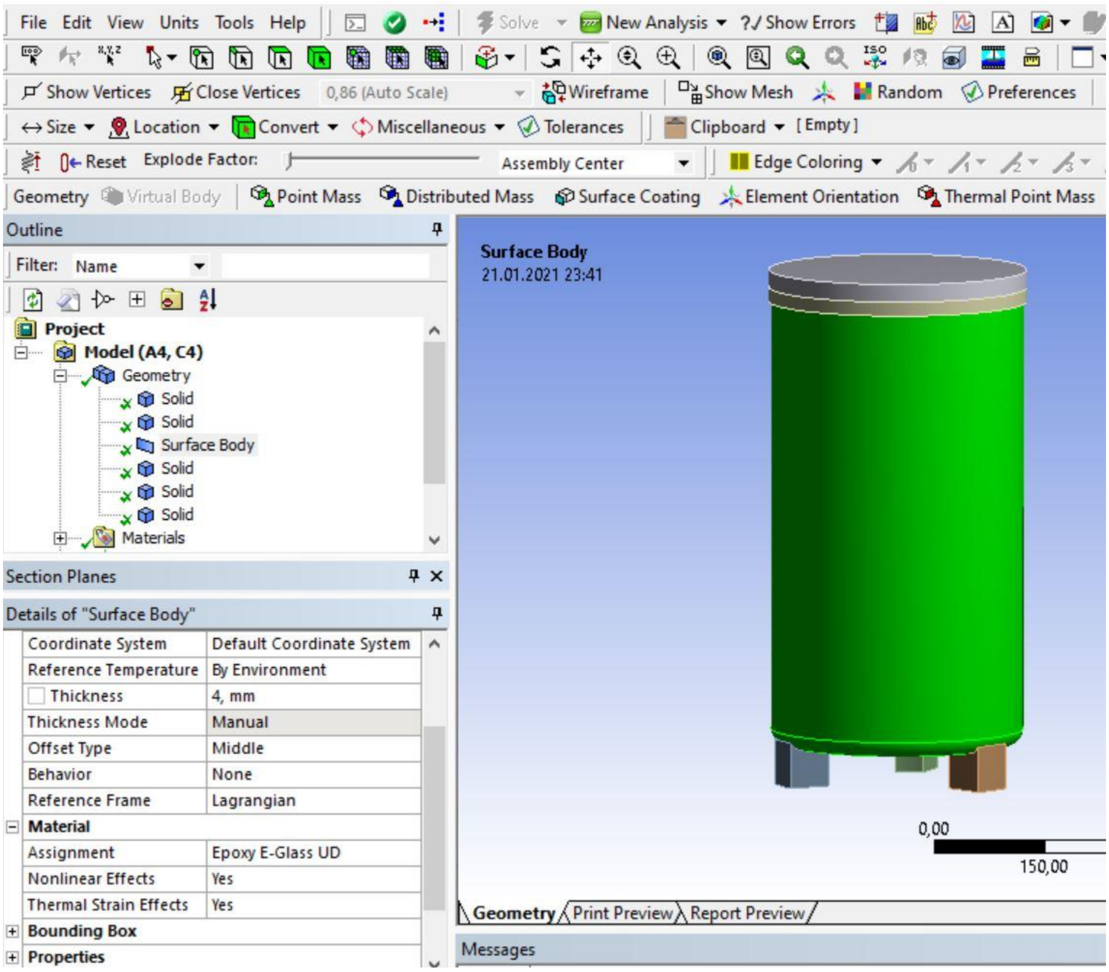

Figure 3.12. Separator Vessel Model Ansys Workbench Interface

As can be seen in Figure 3.13, by selecting Fabric.1 from Material Data> Fabrics section and Stackup.1 from the Stackups section, the layer thickness, material property, total thickness, and orientation angle of the pressure vessel are shown.

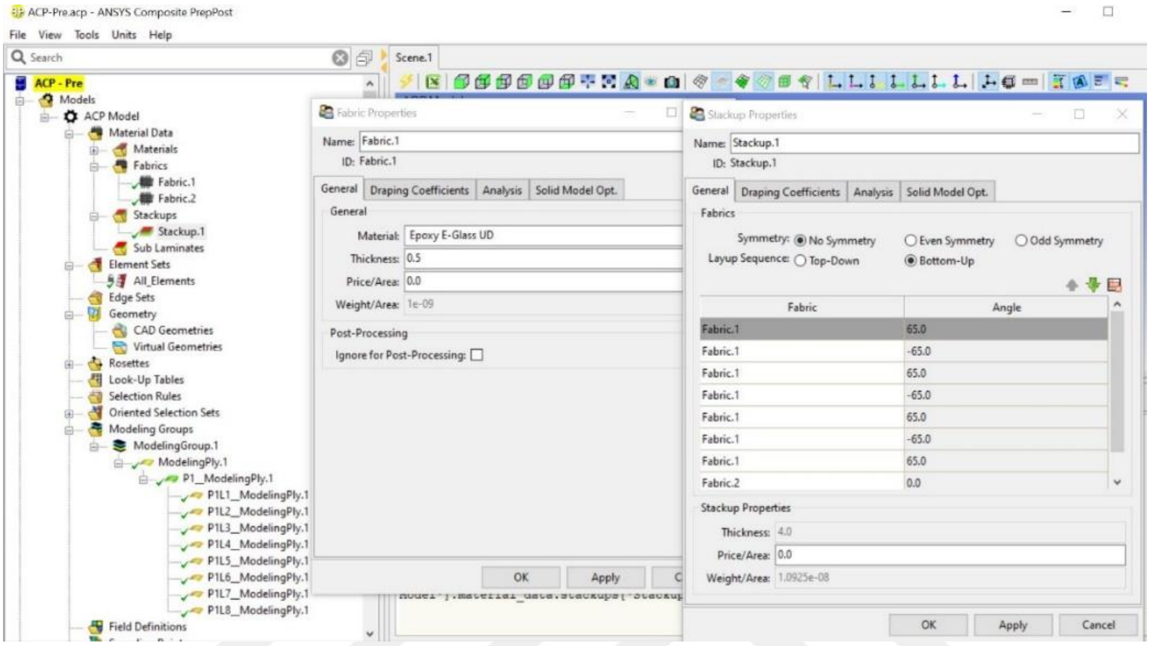

Figure 3.13. Display of material property, layer thickness, and orientation angles

As can be seen in Figure 3.14, after the geometry conditions and element properties are completed, the mesh operation is precisely adjusted. The pressure vessel model is divided into very small areas called hexahedron elements for 0.5 mm structural steel covered with 3.5 mm composite material.

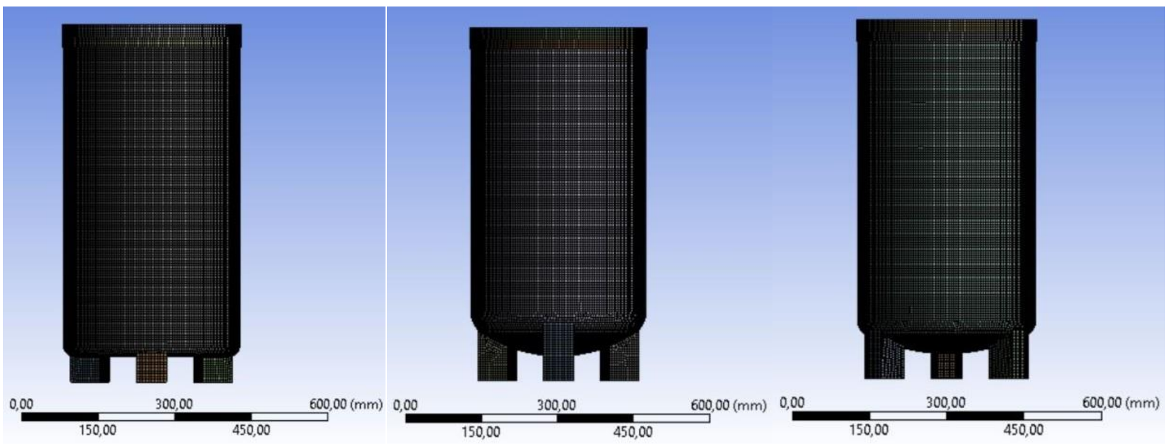

Figure 3.14. Meshed CAD Model for 0.5 mm structure steel.

Table 3.6 shows the number of nodes and the number of elements for 0.5 mm structure steels in each case.

Table 3.6. Mesh data for 0.5 mm structure steel covered with composite materials.

0.5 mm Structure Steel	Number of Nodes	Number of Elements
Flat Dish End	255137	77497
Elliptical Dish End	262123	77323
Torispheric Dish End	259164	77324

As seen in Figure 3.15, to get the boundary conditions; Analysis Settings> Insert> Pressure is selected. The designed pressure vessel is cross-sectioned since it is necessary to apply internal pressure. The pressure is applied to the inner surface of the vessel. The pressure value was entered into the Magnitude part as the test pressure, 1.5 times the working pressure.

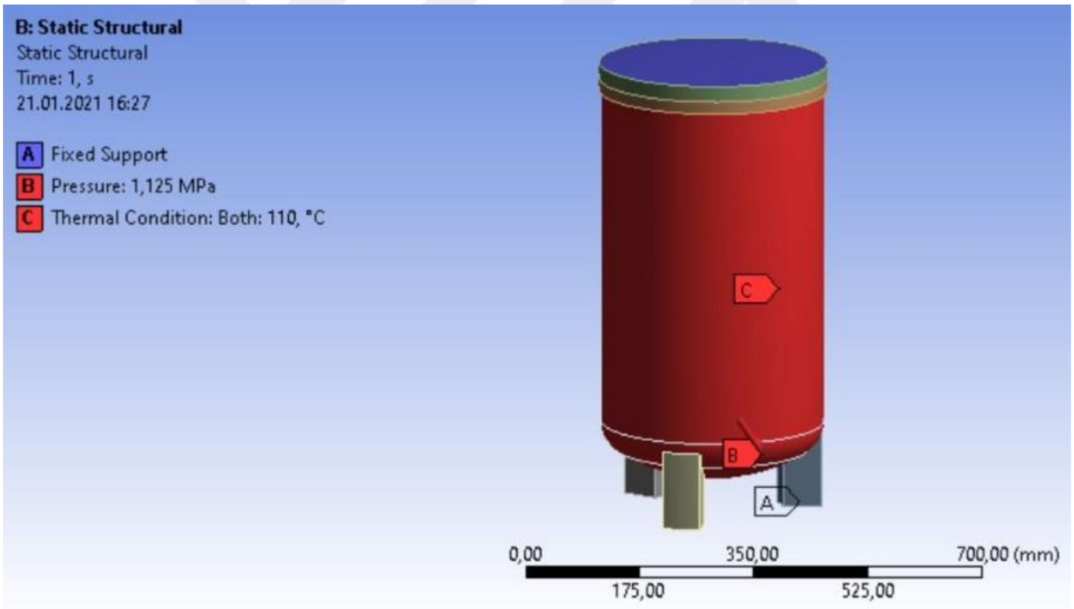

Figure 3.15. Boundary Conditions

Separator oil tanks are fixed to the chassis from leg supports in compressor systems. As it can be seen in Figure 3.16, taking boundary conditions has been done from Analysis Settings> Insert> Fixed Support menu.

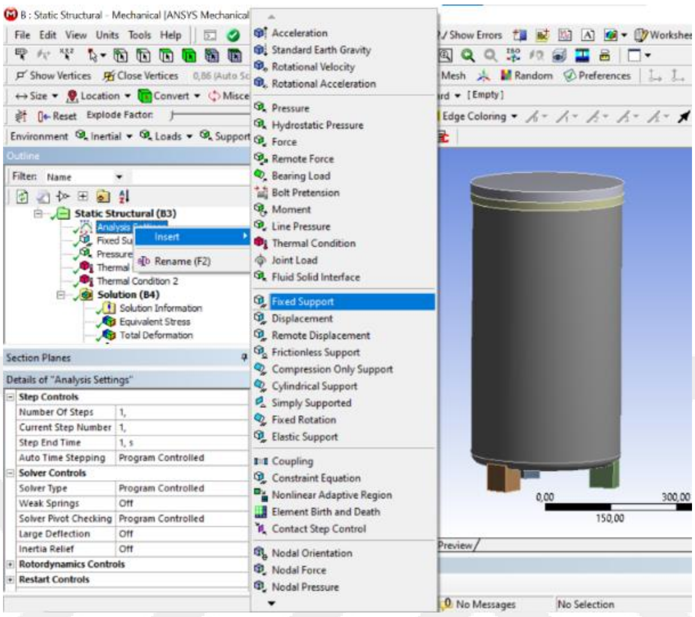

Figure 3.16. Choosing Fixed Support

In Figure 3.17, the stresses and total deformations resulting from the finite element analysis are shown.

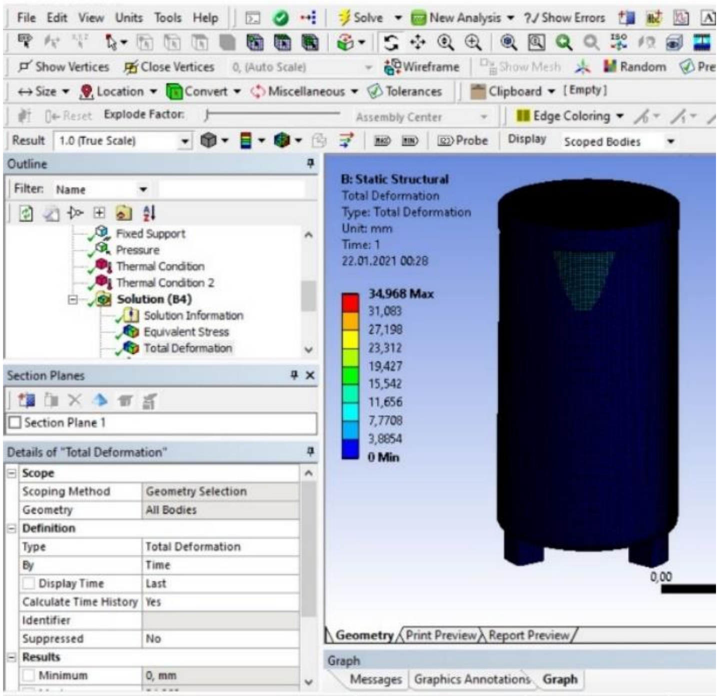

Figure 3.17. Getting results from the finite element analysis

First ply failure (FPF) is a widely used method for estimating the strength of a composite. The method determines the stresses generated in each layer using the laminate properties and loads through Classical Laminate Theory [41]. Thanks to the fracture criteria and the stress information in each layer of the composite material, the load at which any of the layers will fail can be determined. With FPF, the first layer failure of the laminate gives us the information that the composite has failed. Therefore, FPF stresses were investigated in this study. Figure 3.18 shows how to read these stress values using the finite element method.

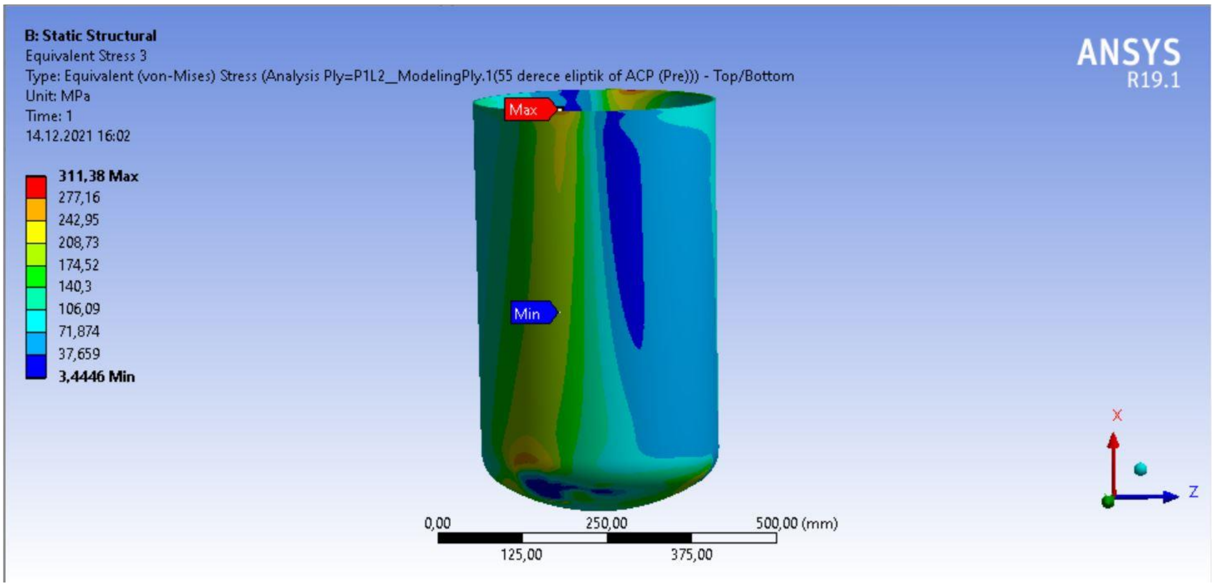

Figure 3.18. Reading first-ply equivalent stress values

First ply failure (fpf) formula is defined below.

$$I_{fpf} = (\frac{\sigma_1}{S_L^2})^2 \frac{\sigma_1 \sigma_2}{S_L^2} + (\frac{\sigma_2}{S_T^2})^2 + (\frac{\tau_{12}}{S_{LT}^2})^2 \geq 1 \quad (12)$$

I_{fpf} is the first-ply failure index, 1 is in the fiber's longitudinal direction, 2 is transverse to the fiber's axis. The values of the strength used in this equation are chosen depending on the direction of σ1 and σ2. For example, if σ_1 is tensile is used, and if σ_2 is compressive would be used. Subscript "L" represents the longitudinal direction and "T " transverse direction. Superscript "+" represents tension and "−" denotes compression. SLT is in-plane shear strength [41].

4. RESULTS AND DISCUSSIONS

In this study, a pressure vessel model was designed using the AUTODESK INVENTOR solid model program. With the help of ANSYS analysis, the material properties, wall thickness, number of layers, orientation angles, and boundary conditions of the pressure vessel model were entered, and stresses and total deformations were determined.

The separator tank body sheet plate is covered with glass fiber/epoxy, carbon fiber/epoxy, and kevlar fiber/epoxy composite materials. Composite coatings were designed with 7 layers and each layer thickness to be 0.5 mm. Analysis studies were carried out using different winding angles (35°/-35°, 45°/-45°, 55°/-55°, and 65°/-65°) and different dish ends at 110 °C constant temperature and different pressure values. By examining the stresses and total deformations obtained as a result of the analysis, the most suitable head type, composite material, and winding angle for different pressures were decided.

Also, the stress and total deformation values of the separator tank body sheet plate of 4 mm thickness and 2 different types (P265GH and P235GH) were examined at 110 °C constant temperature and using different pressure values and different dish ends. It has been determined which steel sheet and which head type would be appropriate for different internal pressures. All the analysis results made with the finite element method are given below in tables and graphics.

Table 4.1. Total deformations and first-ply equivalent stresses of vessel with flat dish end w.r.t. the orientation angle and hydrostatic pressure.

TYPE	LAYER ORIENTATION (degree)	HYDROSTATIC PRESSURE (bar)	TOTAL DEFORMATION (mm)	FIRST-PLY EQUIVALENT STRESS (MPa)
Carbon Fiber/Epoxy	$[35/-35]_7$	11.25	13.559	1020.10
Carbon Fiber/Epoxy	$[35/-35]_7$	15.0	18.097	1355.80
Carbon Fiber/Epoxy	$[35/-35]_7$	19.5	23.544	1758.60
Glass Fiber/Epoxy	$[35/-35]_7$	11.25	19.633	414.60
Glass Fiber/Epoxy	$[35/-35]_7$	15.0	26.187	554.84
Glass Fiber/Epoxy	$[35/-35]_7$	19.5	34.051	723.13
Kevlar Fiber/Epoxy	$[35/-35]_7$	11.25	6.8875	624.76
Kevlar Fiber/Epoxy	$[35/-35]_7$	15.0	9.1993	819.51
Kevlar Fiber/Epoxy	$[35/-35]_7$	19.5	11.9730	1081.20
Carbon Fiber/Epoxy	$[45/-45]_7$	11.25	12.988	939.43
Carbon Fiber/Epoxy	$[45/-45]_7$	15.0	17.320	1247.70
Carbon Fiber/Epoxy	$[45/-45]_7$	19.5	22.518	1617.70
Glass Fiber/Epoxy	$[45/-45]_7$	11.25	19.197	415.56
Glass Fiber/Epoxy	$[45/-45]_7$	15.0	25.599	550.08
Glass Fiber/Epoxy	$[45/-45]_7$	19.5	33.280	711.54
Kevlar Fiber/Epoxy	$[45/-45]_7$	11.25	6.9017	618.24
Kevlar Fiber/Epoxy	$[45/-45]_7$	15.0	9.2150	834.37
Kevlar Fiber/Epoxy	$[45/-45]_7$	19.5	11.9910	1097.80
Carbon Fiber/Epoxy	$[55/-55]_7$	11.25	13.229	886.34
Carbon Fiber/Epoxy	$[55/-55]_7$	15.0	17.644	1177.60
Carbon Fiber/Epoxy	$[55/-55]_7$	19.5	22.942	1527.10
Glass Fiber/Epoxy	$[55/-55]_7$	11.25	19.396	426.21
Glass Fiber/Epoxy	$[55/-55]_7$	15.0	25.863	566.16
Glass Fiber/Epoxy	$[55/-55]_7$	19.5	33.622	734.13
Kevlar Fiber/Epoxy	$[55/-55]_7$	11.25	6.9097	638.93
Kevlar Fiber/Epoxy	$[55/-55]_7$	15.0	11.3700	848.42
Kevlar Fiber/Epoxy	$[55/-55]_7$	19.5	11.9970	1112.10
Carbon Fiber/Epoxy	$[65/-65]_7$	11.25	14.317	1050.20
Carbon Fiber/Epoxy	$[65/-65]_7$	15.0	19.108	1391.80
Carbon Fiber/Epoxy	$[65/-65]_7$	19.5	24.857	1801.70
Glass Fiber/Epoxy	$[65/-65]_7$	11.25	20.168	462.35
Glass Fiber/Epoxy	$[65/-65]_7$	15.0	26.896	616.53
Glass Fiber/Epoxy	$[65/-65]_7$	19.5	34.968	801.56
Kevlar Fiber/Epoxy	$[65/-65]_7$	11.25	6.9171	647.91
Kevlar Fiber/Epoxy	$[65/-65]_7$	15.0	9.2282	867.81
Kevlar Fiber/Epoxy	$[65/-65]_7$	19.5	12.0010	1134.10

Table 4.2. Total deformations and first-ply equivalent stresses of vessel with elliptical dish end w.r.t. the orientation angle and hydrostatic pressure.

TYPE	LAYER ORIENTATION (degree)	HYDROSTATIC PRESSURE (bar)	TOTAL DEFORMATION (mm)	FIRST-PLY EQUIVALENT STRESSES (MPa)
Carbon Fiber/Epoxy	$[35/-35]_7$	11.25	2.9719	240.28
Carbon Fiber/Epoxy	$[35/-35]_7$	15.0	3.2713	281.80
Carbon Fiber/Epoxy	$[35/-35]_7$	19.5	3.6373	331.66
Glass Fiber/Epoxy	$[35/-35]_7$	11.25	1.7503	105.14
Glass Fiber/Epoxy	$[35/-35]_7$	15.0	2.0951	128.38
Glass Fiber/Epoxy	$[35/-35]_7$	19.5	2.5213	156.27
Kevlar Fiber/Epoxy	$[35/-35]_7$	11.25	2.1294	310.38
Kevlar Fiber/Epoxy	$[35/-35]_7$	15.0	2.1229	334.03
Kevlar Fiber/Epoxy	$[35/-35]_7$	19.5	2.1244	363.20
Carbon Fiber/Epoxy	$[45/-45]_7$	11.25	1.5023	229.32
Carbon Fiber/Epoxy	$[45/-45]_7$	15.0	1.8894	261.69
Carbon Fiber/Epoxy	$[45/-45]_7$	19.5	2.3606	300.55
Glass Fiber/Epoxy	$[45/-45]_7$	11.25	1.5115	101.84
Glass Fiber/Epoxy	$[45/-45]_7$	15.0	1.9108	124.00
Glass Fiber/Epoxy	$[45/-45]_7$	19.5	2.3958	151.65
Kevlar Fiber/Epoxy	$[45/-45]_7$	11.25	1.0039	289.02
Kevlar Fiber/Epoxy	$[45/-45]_7$	15.0	1.0747	312.36
Kevlar Fiber/Epoxy	$[45/-45]_7$	19.5	1.1715	341.24
Carbon Fiber/Epoxy	$[55/-55]_7$	11.25	4.0827	240.82
Carbon Fiber/Epoxy	$[55/-55]_7$	15.0	4.8121	272.59
Carbon Fiber/Epoxy	$[55/-55]_7$	19.5	5.6889	311.38
Glass Fiber/Epoxy	$[55/-55]_7$	11.25	2.6552	102.65
Glass Fiber/Epoxy	$[55/-55]_7$	15.0	3.2695	119.58
Glass Fiber/Epoxy	$[55/-55]_7$	19.5	4.0098	146.66
Kevlar Fiber/Epoxy	$[55/-55]_7$	11.25	1.9013	284.79
Kevlar Fiber/Epoxy	$[55/-55]_7$	15.0	2.0059	319.00
Kevlar Fiber/Epoxy	$[55/-55]_7$	19.5	2.1353	360.21
Carbon Fiber/Epoxy	$[65/-65]_7$	11.25	5.6487	243.34
Carbon Fiber/Epoxy	$[65/-65]_7$	15.0	6.5477	274.71
Carbon Fiber/Epoxy	$[65/-65]_7$	19.5	7.6276	312.38
Glass Fiber/Epoxy	$[65/-65]_7$	11.25	3.3913	102.70
Glass Fiber/Epoxy	$[65/-65]_7$	15.0	4.1262	119.12
Glass Fiber/Epoxy	$[65/-65]_7$	19.5	5.0107	147.77
Kevlar Fiber/Epoxy	$[65/-65]_7$	11.25	2.8268	290.99
Kevlar Fiber/Epoxy	$[65/-65]_7$	15.0	2.8084	325.53
Kevlar Fiber/Epoxy	$[65/-65]_7$	19.5	2.8994	368.06

Table 4.3. Total deformations and first-ply equivalent stresses of vessel with torispheric dish end w.r.t. the orientation angle and hydrostatic pressure.

Table 4.4. Stress and total deformation values at different pressures on separator tank with flat dish end and P265GH and P235GH sheet plates.

TYPE	LAYER ORIENTATION (degree)	HYDROSTATIC PRESSURE (bar)	TOTAL DEFORMATION (mm)	FIRST-PLY EQUIVALENT STRESSES (MPa)
Carbon Fiber/Epoxy	$[35/-35]_7$	11.25	0.78541	286.87
Carbon Fiber/Epoxy	$[35/-35]_7$	15.0	0.95287	341.86
Carbon Fiber/Epoxy	$[35/-35]_7$	19.5	1.15390	407.90
Glass Fiber/Epoxy	$[35/-35]_7$	11.25	0.94740	125.44
Glass Fiber/Epoxy	$[35/-35]_7$	15.0	1.18030	153.93
Glass Fiber/Epoxy	$[35/-35]_7$	19.5	1.46010	188.62
Kevlar Fiber/Epoxy	$[35/-35]_7$	11.25	2.04890	306.21
Kevlar Fiber/Epoxy	$[35/-35]_7$	15.0	2.07890	337.96
Kevlar Fiber/Epoxy	$[35/-35]_7$	19.5	2.12240	377.16
Carbon Fiber/Epoxy	$[45/-45]_7$	11.25	0.69892	245.26
Carbon Fiber/Epoxy	$[45/-45]_7$	15.0	0.86363	297.50
Carbon Fiber/Epoxy	$[45/-45]_7$	19.5	1.06130	360.22
Glass Fiber/Epoxy	$[45/-45]_7$	11.25	0.92967	120.75
Glass Fiber/Epoxy	$[45/-45]_7$	15.0	1.16240	148.99
Glass Fiber/Epoxy	$[45/-45]_7$	19.5	1.44170	182.88
Kevlar Fiber/Epoxy	$[45/-45]_7$	11.25	0.97497	294.93
Kevlar Fiber/Epoxy	$[45/-45]_7$	15.0	1.03070	325.96
Kevlar Fiber/Epoxy	$[45/-45]_7$	19.5	1.10930	364.93
Carbon Fiber/Epoxy	$[55/-55]_7$	11.25	0.74813	259.53
Carbon Fiber/Epoxy	$[55/-55]_7$	15.0	0.91345	313.26
Carbon Fiber/Epoxy	$[55/-55]_7$	19.5	1.11350	377.79
Glass Fiber/Epoxy	$[55/-55]_7$	11.25	0.94063	123.91
Glass Fiber/Epoxy	$[55/-55]_7$	15.0	1.17500	152.94
Glass Fiber/Epoxy	$[55/-55]_7$	19.5	1.45670	187.80
Kevlar Fiber/Epoxy	$[55/-55]_7$	11.25	1.86970	285.06
Kevlar Fiber/Epoxy	$[55/-55]_7$	15.0	1.89540	318.06
Kevlar Fiber/Epoxy	$[55/-55]_7$	19.5	2.01230	359.24
Carbon Fiber/Epoxy	$[65/-65]_7$	11.25	0.90971	264.21
Carbon Fiber/Epoxy	$[65/-65]_7$	15.0	1.09010	321.54
Carbon Fiber/Epoxy	$[65/-65]_7$	19.5	1.31080	390.41
Glass Fiber/Epoxy	$[65/-65]_7$	11.25	0.97125	126.02
Glass Fiber/Epoxy	$[65/-65]_7$	15.0	1.21200	155.72
Glass Fiber/Epoxy	$[65/-65]_7$	19.5	1.50110	191.37
Kevlar Fiber/Epoxy	$[65/-65]_7$	11.25	2.96530	286.34
Kevlar Fiber/Epoxy	$[65/-65]_7$	15.0	2.94170	323.94
Kevlar Fiber/Epoxy	$[65/-65]_7$	19.5	2.91820	369.11

FLAT DISH END		Hidrostatic Test Pressure		
		11.25 bar	**15 bar**	**19.5 bar**
P265GH	**Max. Stress (bar)**	1265.7	1247.7	1444
	Max. Total Deformation (mm)	3.0988	4.2148	5.5541
P235GH	**Max. Stress (bar)**	1419.4	1405.2	1466.1
	Max. Total Deformation (mm)	3.0223	4.1167	5.4299

Table 4.5. Stress and total deformation values at different pressures on separator tank with elliptical dish end and P265GH and P235GH sheet plates.

ELLIPTICAL DISH END		Hidrostatic Test Pressure		
		11.25 bar	**15 bar**	**19.5 bar**
P265GH	**Max. Stress (bar)**	1179.7	1174.4	1168.1
	Max. Total Deformation (mm)	0.7152	0.7301	0.7479
P235GH	**Max. Stress (bar)**	1337.8	1335.8	1333.6
	Max. Total Deformation (mm)	0.7382	0.7537	0.7723

Table 4.6. Stress and total deformation values at different pressures on separator tank with torispheric dish end and P265GH and P235GH sheet plates.

TORISPHERIC DISH END		Hidrostatic Test Pressure		
		11.25 bar	**15 bar**	**19.5 bar**
P265GH	**Max. Stress (bar)**	1260.9	1253.9	1245.6
	Max. Total Deformation (mm)	0.7371	0.7518	0.7696
P235GH	**Max. Stress (bar)**	1417.1	1413.8	1409.9
	Max. Total Deformation (mm)	0.7617	0.7772	0.7958

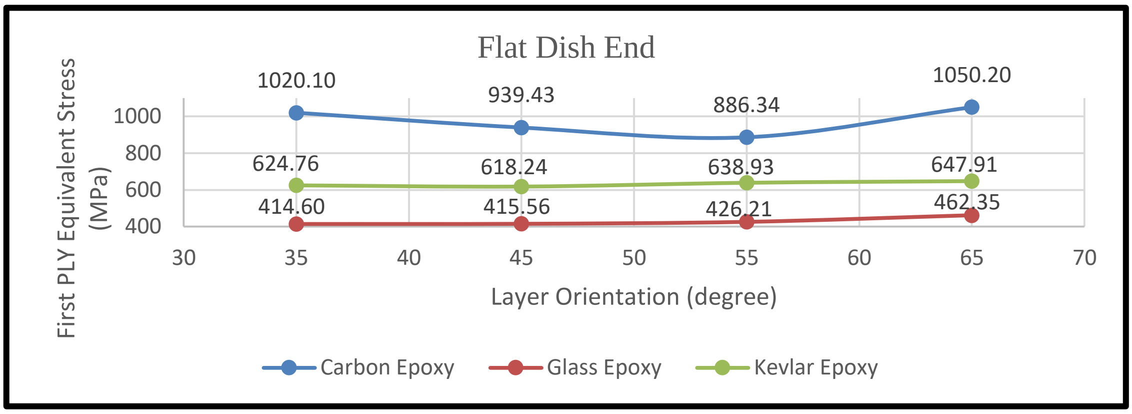

Figure 4.1. The graph of first-ply equivalent stress on the pressure vessel with flat dish end at 11.25 bar hydrostatic pressure.

In Figure 4.1, the lowest first-ply equivalent stress value is 414.60 MPa. It has been seen on the pressure vessel covered with glass fiber/epoxy with the orientation angle of 35°. As a result of the analysis of the separator tank, operating under 11.25 bar pressure, with flat dish end and glass fiber/epoxy composite material, it was observed that the stresses increased as the layer orientation increased from 35° to 65°. The highest stress occurs in the separator tank with a layer orientation of 65° and carbon epoxy composite material.

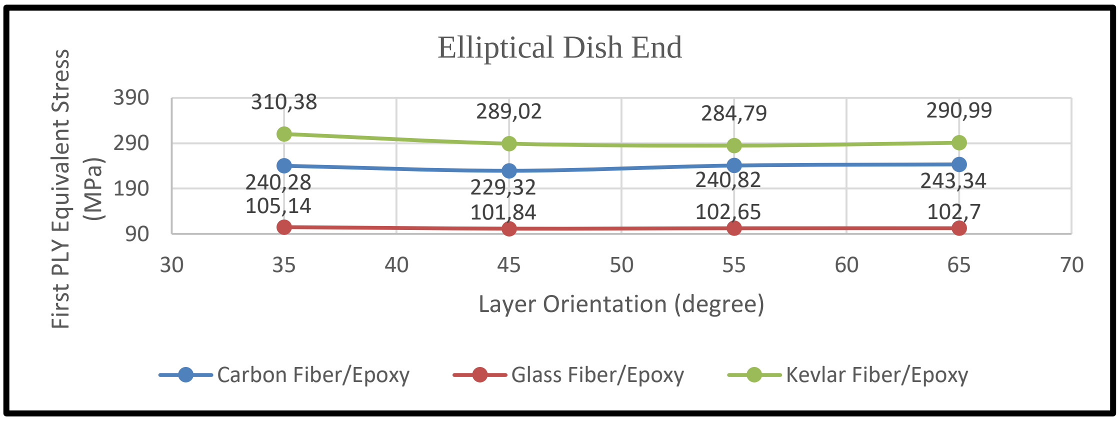

Figure 4.2. The graph of first-ply equivalent stress on the pressure vessel with elliptical dish end at 11.25 bar hydrostatic pressure.

In Figure 4.2, the lowest first-ply equivalent stress value is 101.84 MPa. It has been seen on the pressure vessel covered with glass fiber/epoxy with the orientation angle of 45°. Depending on 11.25 bar pressure and elliptical dish end constants, the highest first-ply equivalent stress value was observed on the separator tank with kevlar fiber/epoxy composite material and a 35° layer orientation.

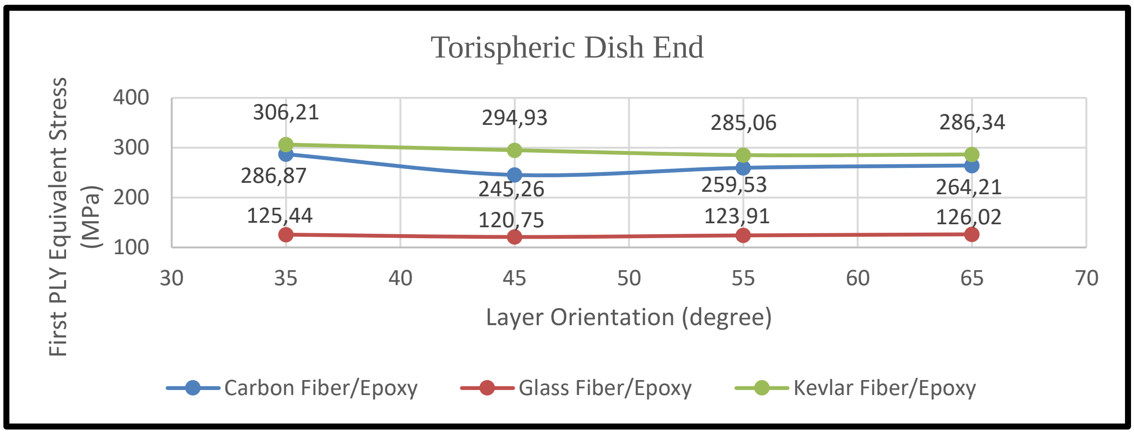

Figure 4.3. The graph of first-ply equivalent stress on the pressure vessel with torispheric dish end at 11.25 bar hydrostatic pressure.

In Figure 4.3, the lowest first-ply equivalent stress value is 120.75 MPa. It has been seen on the pressure vessel covered with glass fiber/epoxy with the orientation angle of 45°. Depending on 11.25 bar pressure and torispheric dish end constants, the highest first-ply equivalent stress value was observed on the separator tank with kevlar fiber/epoxy composite material and a 35° layer orientation.

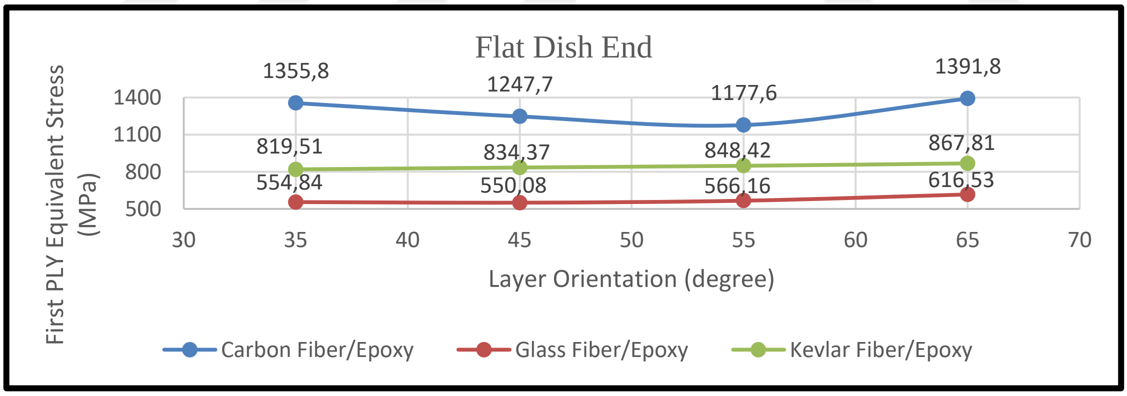

Figure 4.4. The graph of first-ply equivalent stress on the pressure vessel with flat dish end at 15 bar hydrostatic pressure.

In Figure 4.4, the lowest first-ply equivalent stress value is 550.08 MPa. It has been seen on the pressure vessel covered with glass fiber/epoxy with the orientation angle of 45°. Depending on 15 bar pressure and flat dish end constants, the highest first-ply equivalent stress value was observed on the separator tank with carbon fiber/epoxy composite material and a 65° layer orientation. In addition, on the tank wrapped with kevlar fiber/epoxy composite material, it was observed that the stresses increased as the layer orientation increased from 35° to 65°.

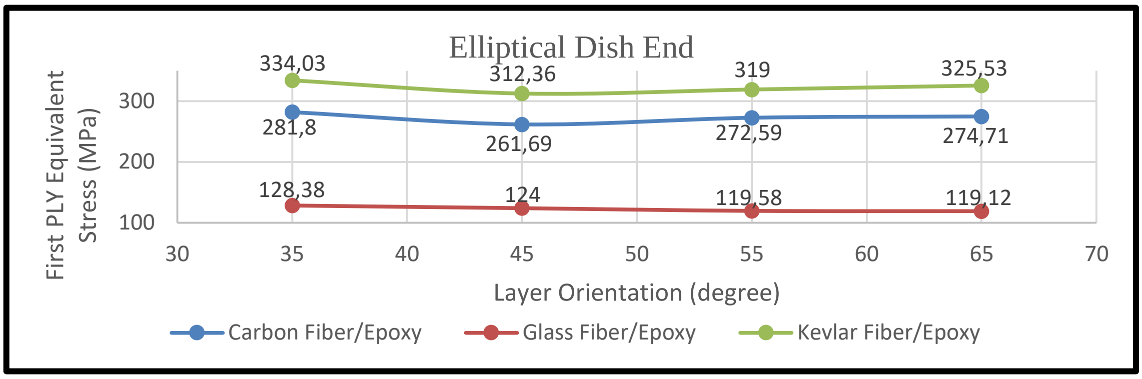

Figure 4.5. The graph of first-ply equivalent stress on the pressure vessel with elliptical dish end at 15 bar hydrostatic pressure.

In Figure 4.5, the lowest first-ply equivalent stress value is 119.12 MPa. It has been seen on the pressure vessel covered with glass fiber/epoxy with the orientation angle of 65°. According to the 15 bar pressure and elliptical dish end constants, the highest first-ply equivalent stress value was observed on the separator tank with kevlar fiber/epoxy composite material and 35° layer orientation. As a result of the analysis using the elliptical dish end, it was observed that the stresses decreased while the layer orientation value for the glass fiber/epoxy composite material increased from 35° to 65°.

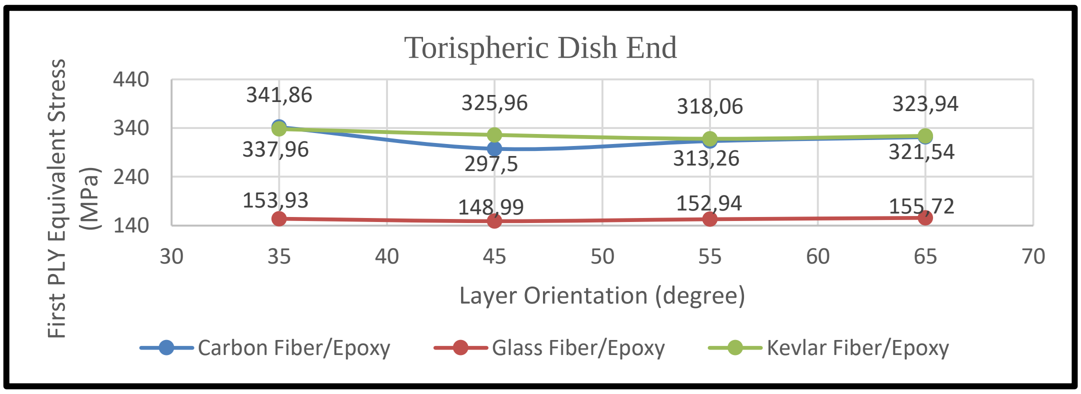

Figure 4.6. The graph of first-ply equivalent stress on the pressure vessel with torispheric dish end at 15 bar hydrostatic pressure.

In Figure 4.6, the lowest first-ply equivalent stress value is 148.99 MPa. It has been seen on the pressure vessel covered with glass fiber/epoxy with the orientation angle of 45°. According to the 15 bar pressure and torispheric dish end constants, the highest first-ply equivalent stress value was observed on the separator tank with carbon fiber/epoxy composite material and 35° layer orientation.

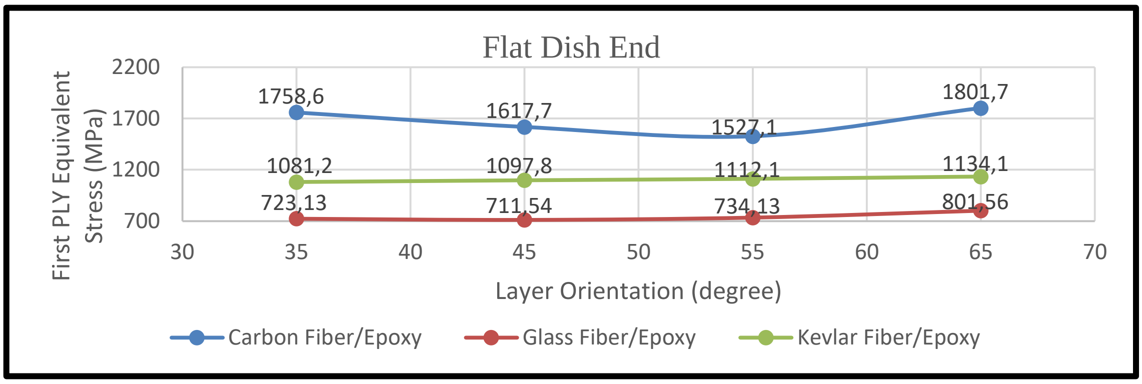

Figure 4.7. The graph of first-ply equivalent stress on the pressure vessel with flat dish end at 19.5 bar hydrostatic pressure.

In Figure 4.7, the lowest first-ply equivalent stress value is 711.54 MPa. It has been seen on the pressure vessel covered with glass fiber/epoxy with the orientation angle of 45°. According to the 19.5 bar pressure and flat dish end constants, the highest first-ply equivalent stress value was observed on the separator tank with carbon fiber/epoxy composite material and 65° layer orientation. As a result of the analysis using the flat dish end, it was observed that the stresses increased while the layer orientation value for the kevlar fiber/epoxy composite material increased from 35° to 65°.

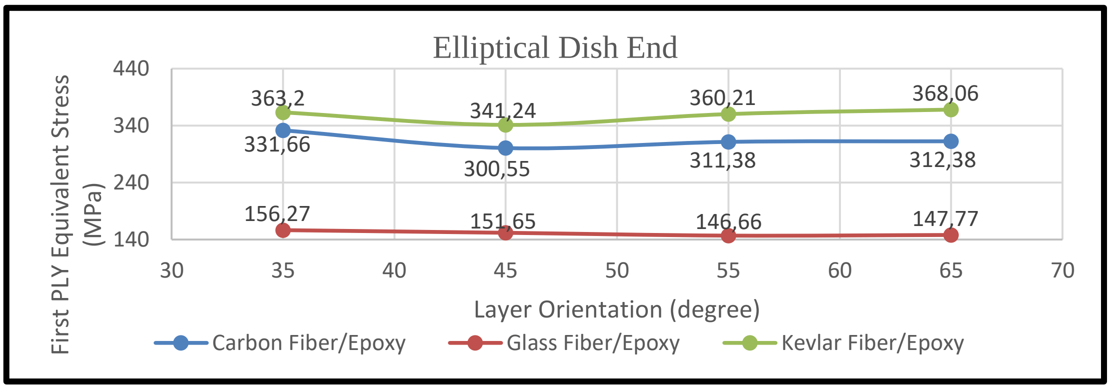

Figure 4.8. The graph of first-ply equivalent stress on the pressure vessel with elliptical dish end at 19.5 bar hydrostatic pressure.

In Figure 4.8, the lowest first-ply equivalent stress value is 146.66 MPa. It has been seen on the pressure vessel covered with glass fiber/epoxy with the orientation angle of 55°. According to the 19.5 bar pressure and elliptical dish end constants, the highest first-ply equivalent stress value was observed on the separator tank with kevlar fiber/epoxy composite material and 65° layer orientation.

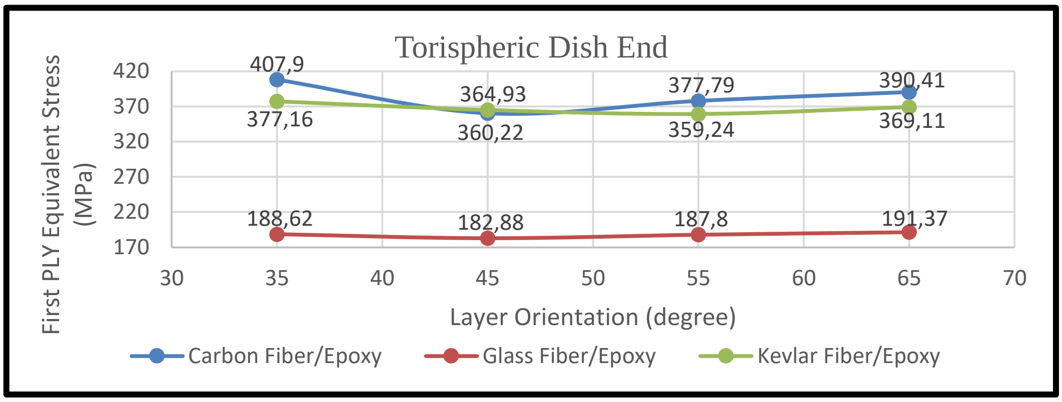

Figure 4.9. The graph of first-ply equivalent stress on the pressure vessel with torispheric dish end at 19.5 bar hydrostatic pressure.

In Figure 4.9, the lowest first-ply equivalent stress value is 182.88 MPa. It has been seen on the pressure vessel covered with glass fiber/epoxy with the orientation angle of 45°. Depending on 19.5 bar pressure and torispheric dish end constants, the highest first-ply equivalent stress value was observed on the separator tank with carbon fiber/epoxy composite material and a 35° layer orientation.

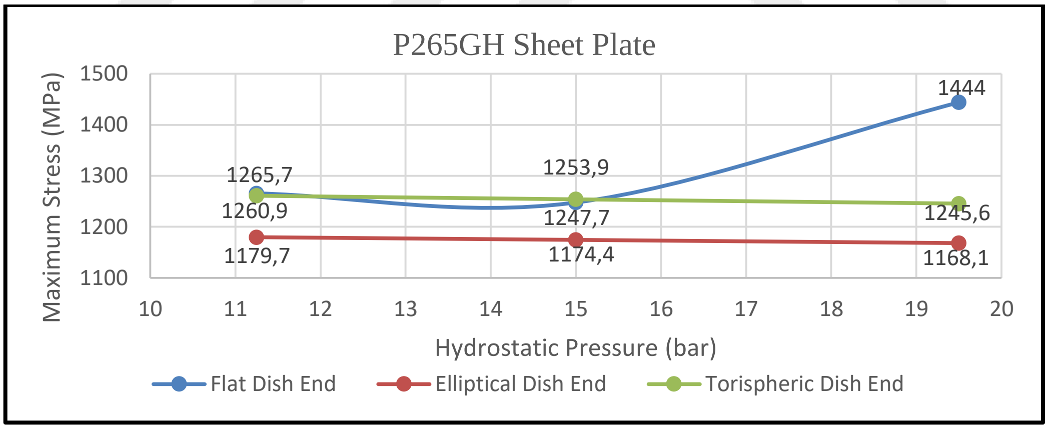

Figure 4.10. The graph of maximum stress on the pressure vessel with P265GH sheet plate for flat, elliptical and torispheric dish ends, at 11.25, 15 and 19.5 bar hydrostatic pressure.

In Figure 4.10, when the sheet plates with 4 mm thickness and a structural property (P265GH) are examined at a constant temperature using different pressure values, it can be observed that the lowest maximum stress value of 1168.1 MPa was obtained from the pressure vessel with an elliptical dish end at 19.5 bar hydrostatic pressure. According to the 19.5 bar pressure and P265GH structure steel constants, the highest first-ply equivalent stress value was observed on the separator tank with a flat dish end.

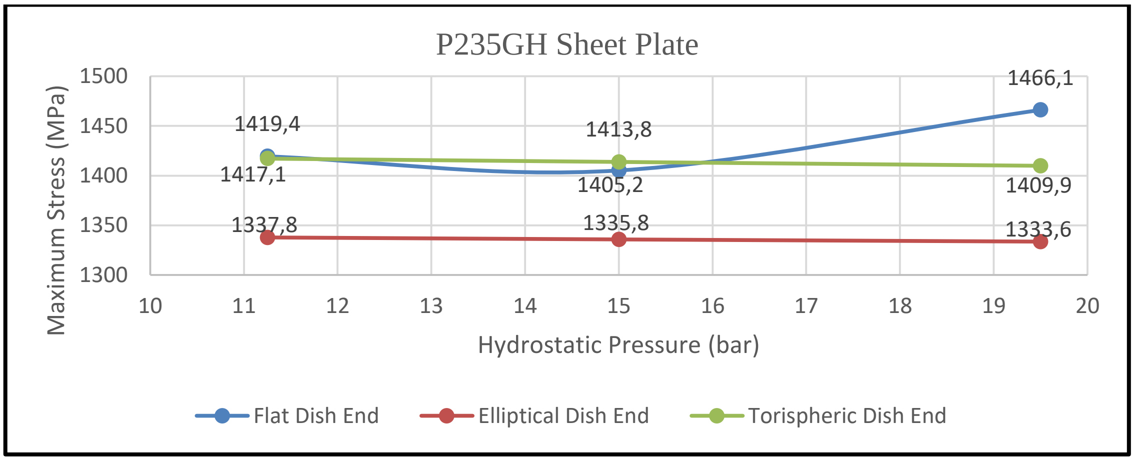

Figure 4.11. The graph of maximum stress on the pressure vessel with P235GH sheet plates, flat, elliptical, and torispheric dish ends, at 11.25, 15, and 19.5 bar hydrostatic pressure.

In Figure 4.11, when the sheet plates with 4 mm thickness and a structural property (P235GH) are examined at a constant temperature using different pressure values, it can be observed that the lowest maximum stress value of 1333.6 MPa was obtained from the pressure vessel with an elliptical dish end at 19.5 bar hydrostatic pressure. According to the 19.5 bar pressure and P235GH structure steel constants, the highest first-ply equivalent stress value was observed on the separator tank with a flat dish end.

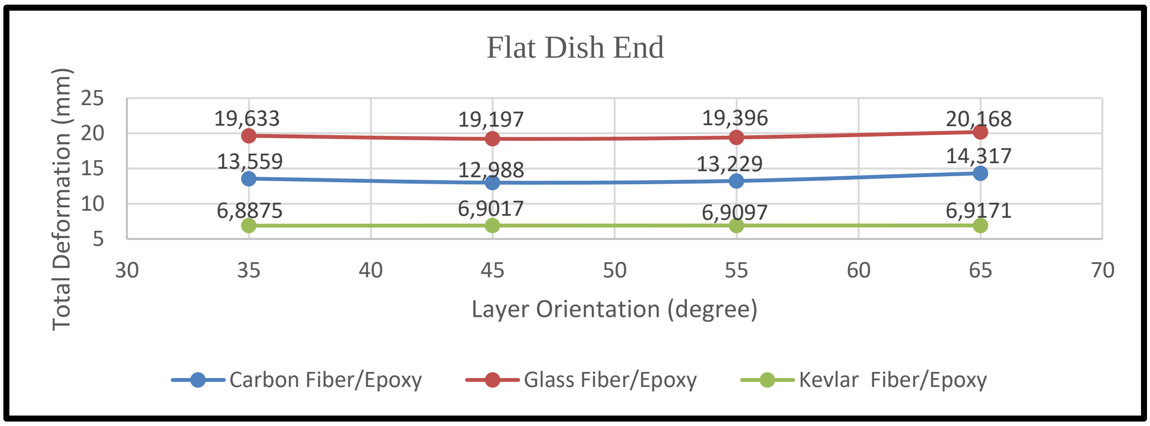

Figure 4.12. The graph of total deformations on pressure vessel with flat dish end at 11.25 bar hydrostatic pressure.

In Figure 4.12 the lowest total deformation value of 6.8875 mm has been obtained from the pressure vessel covered with kevlar fiber/epoxy with an orientation angle of 35°. Depending on 11.25 bar pressure and flat dish end constants, the highest total deformation value was observed on the separator tank with glass fiber/epoxy composite material and a 65° layer orientation.

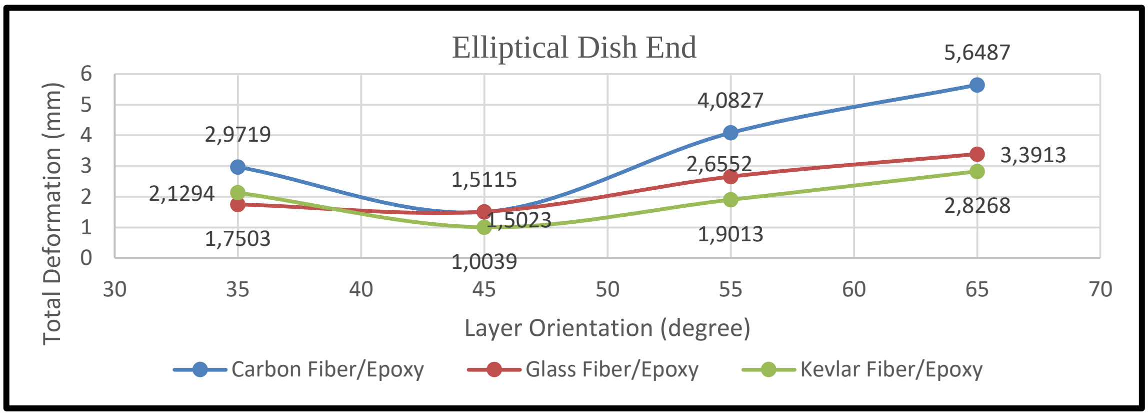

Figure 4.13. The graph of total deformations on pressure vessel with elliptical dish end at 11.25 bar hydrostatic pressure.

In Figure 4.13 the lowest total deformation value is 1.0039 mm. It has been acquired from the pressure vessel covered with kevlar fiber/epoxy with the orientation angle of 45°. Depending on 11.25 bar pressure and elliptical dish end constants, the highest total deformation value was observed on the separator tank with carbon fiber/epoxy composite material and a 65° layer orientation. In addition, a decrease in the total deformations of all material types was determined at 11.25 bar and 45° layer orientation.

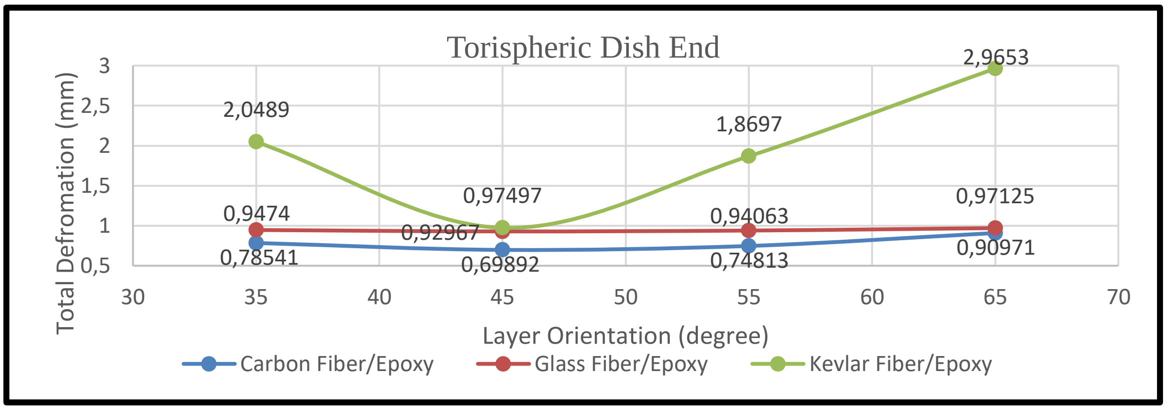

Figure 4.14. The graph of total deformations on pressure vessel with torispheric dish end at 11.25 bar hydrostatic pressure.

In Figure 4.14 the lowest total deformation value is 0.69892 mm. It has been acquired from the pressure vessel covered with carbon fiber/epoxy with the orientation angle of 45°. According to the 11.25 bar pressure and torispheric dish end constants, the highest total deformation value was observed on the separator tank with kevlar fiber/epoxy composite material and 65° layer orientation.

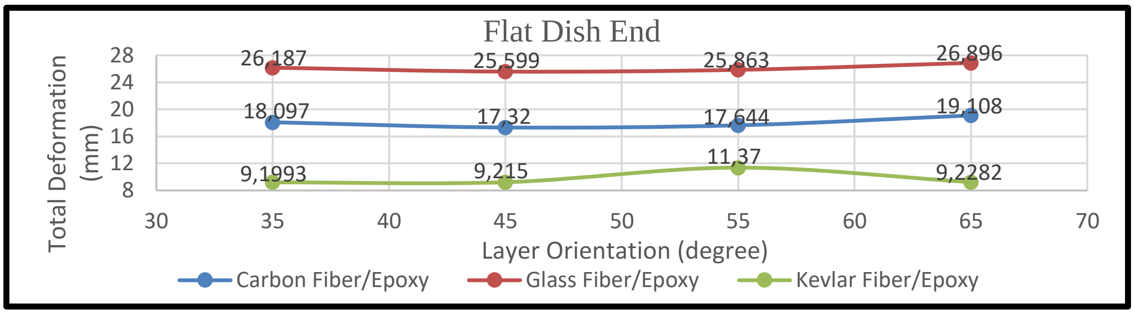

Figure 4.15. The graph of total deformations on pressure vessel with flat dish end at 15 bar hydrostatic pressure.

In Figure 4.15 the lowest total deformation value is 9.1993 mm. It has been acquired from the pressure vessel covered with kevlar fiber/epoxy with the orientation angle of 35°. According to the 15 bar pressure and flat dish end constants, the highest total deformation value was observed on the separator tank with glass fiber/epoxy composite material and 65° layer orientation. When compared to the other composite materials of the pressure vessel designed with flat dish end and kevlar fiber/epoxy, the highest amount of total deformation increase was observed at 55° orientation angle.

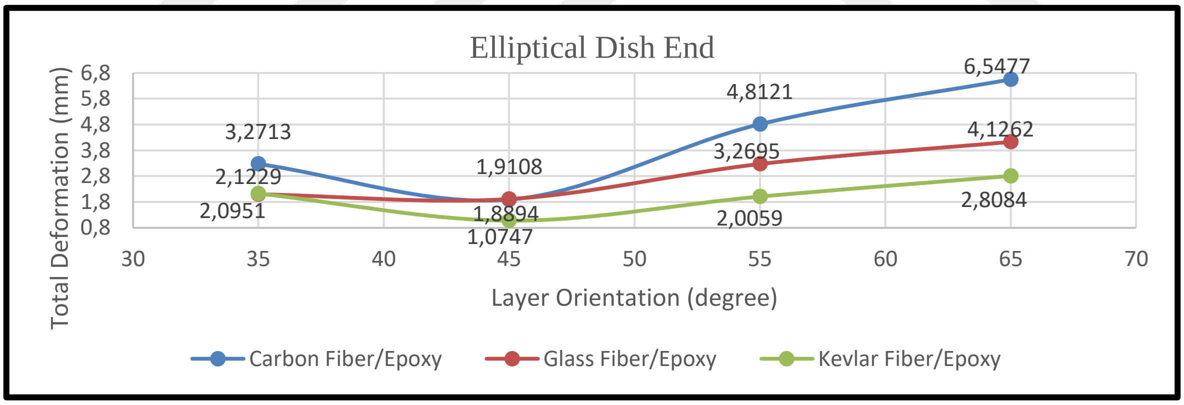

Figure 4.16. The graph of total deformations on pressure vessel with elliptical dish end at 15 bar hydrostatic pressure.

In Figure 4.16 the lowest total deformation value is 1.0747 mm. It has been acquired from the pressure vessel covered with kevlar fiber/epoxy with the orientation angle of 45°. According to the 15 bar pressure and eliptical dish end constants, the highest total deformation value was observed on the separator tank with carbon fiber/epoxy composite material and 65° layer orientation. In addition, a decrease in the total deformations of all material types was determined at 15 bar and 45° layer orientation.

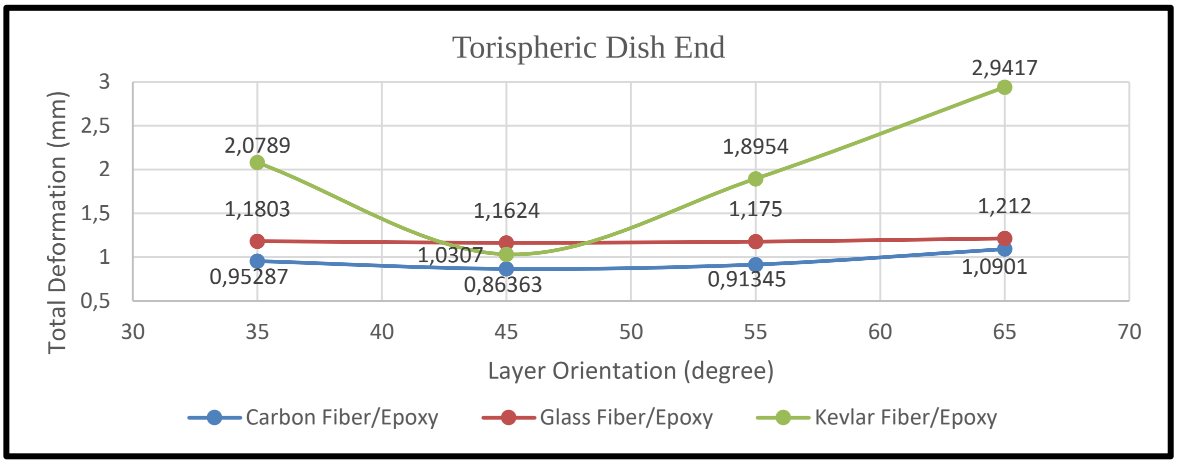

Figure 4.17. The graph of total deformations on pressure vessel with torispheric dish end at 15 bar hydrostatic pressure.

In Figure 4.17 the lowest total deformation value is 0.86363 mm. It has been acquired from the pressure vessel covered with carbon fiber/epoxy with the orientation angle of 45°. Depending on 15 bar pressure and elliptical dish end constants, the highest total deformation value was observed on the separator tank with carbon fiber/epoxy composite material and 65° layer orientation.

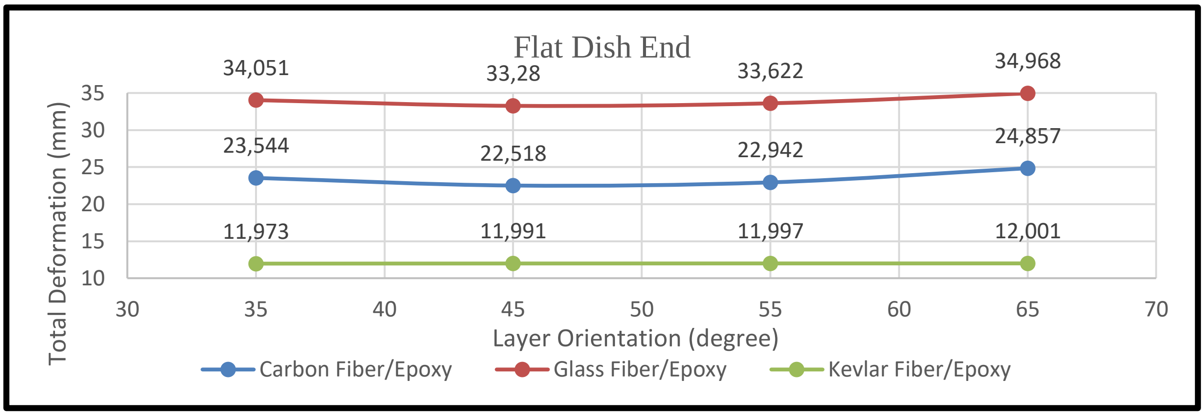

Figure 4.18. The graph of total deformations on pressure vessel with flat dish end at 19.5 bar hydrostatic pressure.

In Figure 4.18 the lowest total deformation value is 11.973 mm. It has been acquired from the pressure vessel covered with kevlar fiber/epoxy with the orientation angle of 35°. Depending on 19.5 bar pressure and flat dish end constants, the highest total deformation value was observed on the separator tank with glass fiber/epoxy composite material and 65° layer orientation.

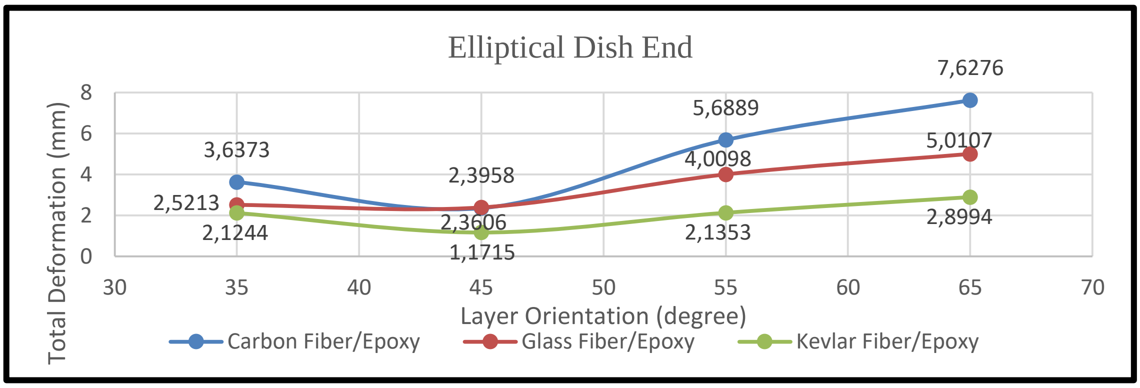

Figure 4.19. The graph of total deformations on pressure vessel with elliptical dish end at 19.5 bar hydrostatic pressure.

In Figure 4.19 the lowest total deformation value is 1.1715 mm. It has been acquired from the pressure vessel covered with kevlar fiber/epoxy with the orientation angle of 45°. Depending on 19.5 bar pressure and elliptical dish end constants, the highest total deformation value was observed on the separator tank with carbon fiber/epoxy composite material and 65° layer orientation.

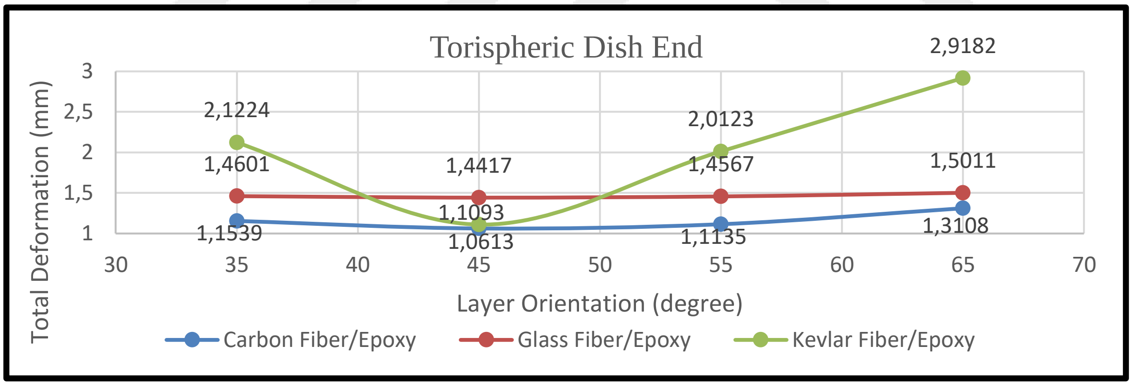

Figure 4.20. The graph of total deformations on pressure vessel with torispheric dish end at 19.5 bar hydrostatic pressure.

In Figure 4.20 the lowest total deformation value is 1.0613 mm. It has been acquired from the pressure vessel covered with carbon fiber/epoxy with the orientation angle of 45°. According to the 19.5 bar pressure and elliptical dish end constants, the highest total deformation value was observed on the separator tank with kevlar fiber/epoxy composite material and 65° layer orientation. The best total deformation results were observed in the pressure vessel designed with kevlar fiber/epoxy composite material at an orientation angle of 45°, compared to the other orientation angles.

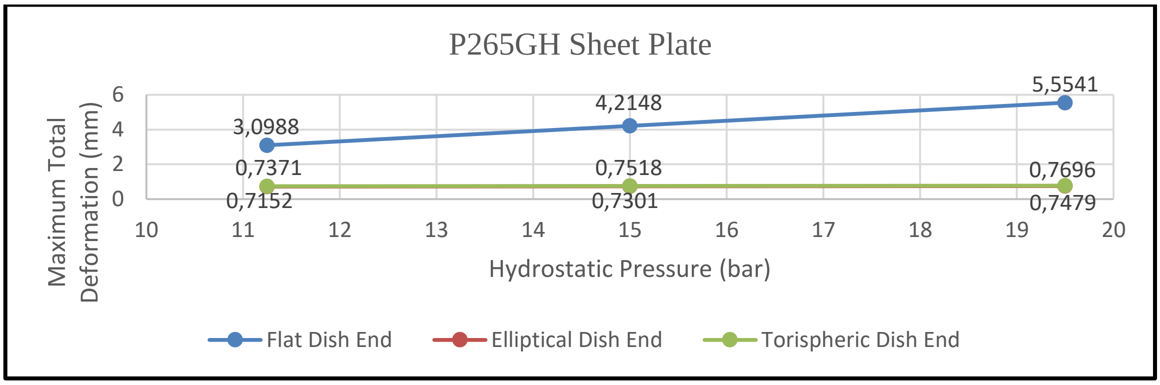

Figure 4.21. The graph of total deformation on pressure vessels with P265GH sheet plate for flat, elliptical and torispheric dish ends, at 11.25, 15 and 19.5 bar hydrostatic pressure.

In Figure 4.21, when the sheet plates with 4 mm thickness and a structural property (P265GH) are examined at a constant temperature using different pressure values, it can be observed that the lowest maximum total deformation value of 0.7152 mm was obtained from the pressure vessel with an elliptical dish end at 11.25 bar hydrostatic pressure. According to the 19.5 bar pressure and P265GH structure steel constants, the highest total deformation value was observed on the separator tank with a flat dish end.

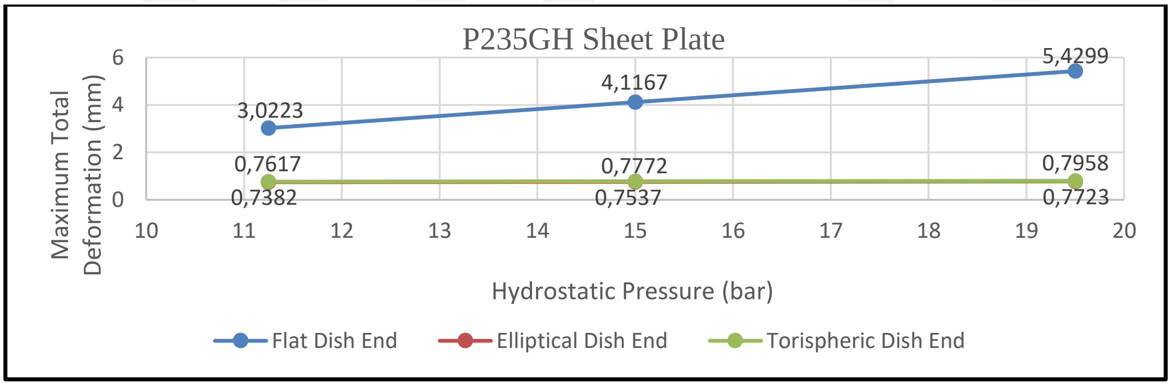

Figure 4.22. The graph of total deformation on pressure vessels with P235GH sheet plates for flat, elliptical and torispheric dish ends, at 11.25, 15 and 19.5 bar hydrostatic pressure.

In Figure 4.22, when the sheet plates with 4 mm thickness and a structural property (P235GH) are examined at a constant temperature using different pressure values, it can be observed that the lowest maximum total deformation value of 0.7382 mm was obtained from the pressure vessel with an elliptical dish end at 11.25 bar hydrostatic pressure. According to the 19.5 bar pressure and P235GH structure steel constants, the highest total deformation value was observed on the separator tank with a flat dish end.

5. CONCLUSIONS

In this study, the analyzes of the separator tank, the base layer of which is 0.5 mm structural steel, and the other layers are covered with three different types of composite materials were calculated using finite element analysis under three different pressure values. Then, stress and deformation analysis of the separator tank, which was designed only with structural steel and had a thickness of 4 mm, was carried out under three different pressure values. It has been observed that the results vary according to the dish ends, composite material types, and orientation angles.

Analyzes were made using three different types of composite materials (carbon, glass, and kevlar fiber/epoxy), four different winding angles (35°/-35°, 45°/-45°, 55°/-55°, and 65°/-65°), three different pressures (11.25, 15, 19.5 bar), and three different dish ends (flat, elliptical, and torispheric).

When the analyzes were examined in the separator tank designed using three different dish ends the highest stresses and total deformations were observed on the separator tank with a flat dish end. The best results were obtained from the separator tanks with an elliptical dish end. According to the results of the finite element analysis of the separator tank, which is designed with both structural steel and composite material, it was determined that the highest stresses and total deformations generally occur in the flat dish end. It was also observed that the stress and deformation values increased as the pressure increased. When all of the results were examined, it was seen that the lowest stress values were obtained in the separator tank with an elliptical dish end coated with glass fiber/epoxy with a 45°/-45° winding angle at 11.25 bar. The lowest total deformation was obtained in the separator tank with torispheric dish end coated with carbon fiber/epoxy with a 45°/-45° winding angle at 11.25 bar.

6. RECOMMENDATIONS

In this thesis, pressure vessels with different dish ends and 4 mm sheet metal (P265GH and P235GH) were designed in various structures using glass, carbon, and kevlar fiber/epoxy materials. Each layer is designed to be 0.5 mm thick. 35°/-35°, 45°/-45°, 55°/-55°, and 65°/-65° angles were used as the winding angle. By applying 11.25, 15 and 19.5 bar pressures to the designed vessels, total deformation and stress values were obtained. Based on these measured data, the optimum winding angle was determined in terms of maximum stresses and total deformation. Vessels can be designed using different design parameters and constraints:

1. Using different pressure values, the maximum strength pressure of the vessels can be determined.
2. Composite vessels can be produced using different materials and the optimum material type can be determined.
3. The optimum number of layers can be determined by changing the number of layers.
4. By using different vessel volumes, the optimum vessel volume can be determined.
5. By using different temperature values, the optimum temperature value can be determined.
6. These designed vessels can be produced by selecting the appropriate production method and subjected to real experimental conditions and the accuracy of the data obtained in the design and theoretical analysis can be supported.

REFERENCES

[1] Bozkurt, S., ‘‘2014/29/AB standartlarına uygun içten basınca maruz kompozit basınçlı kap tasarımı ve analizi’’, Yüksek Lisans Tezi, *Bingöl Üniversitesi, Fen Bilimleri Enstitüsü***,** Bingöl, pp-106 (2018).

[2] Sancaklı, İ., ‘‘Basınçlı kap konstrüksiyonlarına etki eden parametrelerin incelenmesi ve tasarımı’’, Yüksek Lisans Tezi, *Yıldız Teknik Üniversitesi, Fen Bilimleri Enstitüsü***,** İstanbul, 1-83 (2017).

[3] Balcı, A., ‘‘Basınçlı kaplarda malzeme seçimi için karar destek sisteminin geliştirilmesi’’, Yüksek Lisans Tezi, *Gazi Üniversitesi, Fen Bilimleri Enstitüsü***,** Ankara,1-128 (2014).

[4] Mestan, F., ‘‘ Basınçlı kapların deneysel ve teorik olarak incelenmesi’’, Yüksek Lisans Tezi, *Hava Harp Okulu, Havacılık ve Uzay Teknolojileri Enstitüsü***,** İstanbul, 1-84 (2010).

[5] Usta, M., ‘‘Birbirinden farklı kalın cidarlı basınçlı kaplarda kaynaklı bölgelerin TS 17020 uygunluğunun araştırılması’’, Yüksek Lisans Tezi, *Namık Kemal Üniversitesi, Fen Bilimleri Enstitüsü***,** Tekirdağ, 1-52 (2011).

[6] Kandaz, M., ‘‘Computer aided design and structural analysis of pressure vessels’’, Thesis, *Middle East Thecnical Universty, The Graduate School of Natural and Applied Sciences***,** Ankara, 1-114 (2006).

[7] Yıldırım, F., ‘‘İnce cidarlı basınçlı kapların yük altındaki mekanik davranışlarının deneysel ve sayısal analizi’’, Yüksek Lisans Tezi, *Karabük Üniversitesi, Fen Bilimleri Enstitüsü***,** Karabük, 1-77 (2012).

[8] Tjelta, F., ‘‘A comparison study of pressure vessel design using different standards’’Master Thesis, *University of Stavanger, Faculty of Science and Technology***,** Stavanger, 1-119 (2012).

[9] Raparla, S.K. and Seshaiah, T. (2012). Design and analysis of multilayer high pressure vessels, International Journal of Engineering Research and Applications, 2(1),355-361.

[10] Ahmed, M., Khan, R.U., Badshah, S. and Jan, S. (2014). Finite element investigation of geometry effect on pressure vessel under combined structural and thermal loads, International Journal of Engineering and Advanced Technology, 4(2), 118-124.

[11] Yaylağan, E. (2010). Determination of Composite Pressure Vessels Under Varius Loadings, Dokuz Eylül University Graduate School of Natural and Applied Sciences, İzmir.

[12] Baba, S. (2013). Anizotropik Kalın Cidarlı Basınçlı Kapların Serbest ve Zorlanmış Titreşim Davranışı, T.C. Ondokuz Mayıs Üniversitesi Fen Bilimleri Enstitüsü Makina Mühendisliği Anabilim Dalı, Samsun.

[13] Wadkar, V.V., Malgave, S.S., Patil, D.D., Bhore, H.S. and Gavade, P.P. (2015). Design and analysis of pressure vessel using ANSYS, Journal of Mechanical Engineering and Technology,3(2), 01-13.

[14] Kolekar, D. and Jewargi, S.S. (2015). Stress analysis of pressure vessel with different type of end connections by FEA, International Journal of Innovative Research in Science, 04(5), 2769-2775.

[15] Pehlivan, A. (2017). Elyaf Sarma ile Üretilen Kompozit Yapıdaki Basınçlı Kapların Değişik Yüklemelerde Modellenmesi, İstanbul Teknik Üniversitesi Bilişim Enstitüsü Hesaplamalı Bilim ve Mühendislik Anabilim Dalı, İstanbul.

[16] Poojary, A.T., Jagannath, S., Nayak, R., and Kini, C.R. (2015). Modelling and Equivalent Stress Analysis of Flat Dish End Pressure Vessel, International Journal of Current Engineering and Technology, 5(5), 3110-3114.

[17] Sinha, M. and Pandit, D. (2012). Design and Burst Pressures Analysis of CFRP Composite Pressure Vessel for Various Fiber Orientations Angles, International Journal of Advances in Engineering Science and Technology, 1(1), 35-40.

[18] Kadam, M., Gopalsamy, B., Bujurke, A.A., Joshi, K.M. (2018). Estimation of static burst pressure in unflawed high-pressure cylinders using nonlinear FEA, Thin-Walled Structures, 126, 79-84.

[19] Li, K., Zheng, J., Zhang, Z., Gu, C., Xu, P. and Chen, Z.(2019). A new formula to predict buckling pressure of steel ellipsoidal head under internal pressure, Thin-Walled Structures, 144, 106311.

[20] Khan, S.M.A. (2010). Stress distributions in a horizontal pressure vessel and the saddle supports, International Journal of Pressure Vessels and Piping, 87 (5), 239-244.

[21] Carbonari, R.C., Muñoz-Rojas, P.A., Andrade, E.Q., Paulino, G.H., Nishimoto, K., Silva, E.C.N., (2011). Design of pressure vessels using shape optimization: An integrated approach, International Journal of Pressure Vessels and Piping, 88 (5-7), 198-212.

[22] Zhang, Q., Wang, Z.W., Tang, C.Y., Hu, D.P., Liu, P.Q., and Xia, L.Z. (2012). Analytical solution of thethermo-mechanical stresses inamultilayeredcomposite pressure vessel considering the influence of the closed ends, International Journal of Pressure Vessels and Piping, 98, 102-110.

[23] Al-Gahtani, H., Khathlan, A., Sunar, M. and Naffa'a M. (2014). Local pressure testing of spherical vessels, International Journal of Pressure Vessels and Piping, 114, 61-68.

[24] Şenalp, A.Z. (2012). Investigation of the effects of perturbation forces to buckling in internally pressurized torispheric pressure vessel heads, Advances in Engineering Software, 45(1), 232-238.

[25] Alcantar, V., Aceves, S.M., Ledesma, E., Ledesma, S. and Aguilera, E. (2017). Optimization of Type 4 composite pressure vessels using genetic algorithms and simulated annealing, International Journal of Hydrogen Energy, 42(24), 15770-15781.

[26] Joshi, H.I. and D Acharya, G. (2018). Numerical investigation of design parameters influences on stress distributions in horizontal multi-saddle cylindrical pressure vessel, Materials Today: Proceedings, 5(9), 19480-19489.

[27] Kumar, A.E., Santosh, R.K., Teja, S.R., Abishek, E. (2018). Static and dynamic analysis of pressure vessels with various stiffeners, Materials Today: Proceedings, 5 (2), 5039-5048.

[28] Alegre, J.M., Bravo, P., Preciado, M. and Solaguren-Beascoa, M. (2010). Simulation procedure of high-pressure vessels using the wire winding technique, Engineering Failure Analysis, 17 (1), 61-69.

[29] Hyder, M.J. and Asif, M. (2008). Optimization of location and size of opening in a pressure vessel cylinder using ANSYS, Engineering Failure Analysis, 15(1), 1-19.

[30] Mhetre, T.V. (2018). "Finite element of composite reactor pressure vessel", Master Thesis, University of Texas at Arlington, Arlington, page 48.

[31] Bouvier, M., Guiheneuf, V. and Jean-marie, A. (2019). Modeling and simulation of a composite high-pressure vessel made of sustainable and renewable alternative fibers, International Journal of Hydrogen Energy, 44 (23), 11970-11978.

[32] Siva kumar, B., Prasanna, P., Sushma, J. and Srikanth, K.P. (2018). Stress analysis and design optimization of a pressure vessel using ansys package, Materials Today: Proceedings, 5 (2), 4551-4562.

[33] Akarsu, M. ‘‘Uniform sıcaklık etkisindeki kompozit plakta ansys programı ile ısıl gerilme analizi’’, Yüksek Lisans Tezi, *Namık Kemal Üniversitesi, Fen Bilimleri Enstitüsü*, Tekirdağ, pp 62 (2013).

[34] Yıldırım, H. ‘‘Değişik kompozit malzemelerin mekanik davranışlarının incelenmesi’’, Yüksek Lisans Tezi, *Fırat Üniversitesi, Fen Bilimleri Enstitüsü*, Elazığ, pp 69 (2009).

[35] https://www.indiamart.com/proddetail/glass-reinforced-epoxy-pipes-4287709155.html. Accessed [16.10.2021]

[36] https://www.protec-arisawa.com/filament-winding-the-key-behind-pressure-vessels-performances/. Accessed [13.11.2021]

[37] https://www.mhoxygen.com/product/kevlar-cylinders/. Accessed [13.11.2021]

[38] https://en.wikipedia.org/wiki/Compressor . Accessed [13.11.2021]

[39] https://www.kartalbombe.com.tr/faaliyetlerimiz/bombe-imalati Accessed [15.11.2021]

[40] https://www.ansys.com/support . Accessed [6.12.2021]

[41] Wu, H.C., Eamon, C.D. (2017). *Strengthening of Concrete Structures Using Fiber Reinforced Polymers (FRP): Design, Construction and Practical Applications*. Woodhead Publishing, United States of America.

[42] https://lngfutures.edu.au/wp-content/uploads/2019/10/Pearce-G.-Design-of-Linerless-Carbon-Fibre-Composite-Pressure-Vessel-for-Cryogenic-Fuel-Tank-Applications.pdf. Accessed [6.12.2021]

[43] Seperator tank. https://yakutkazan.com/urun/seperator-tanklari/2/ . Accessed [10.12.2021]